Title:

The pathogenic Lrrk2-R1441C mutation induces specific deficits modeling the prodromal phase of Parkinson´s Disease in the mouse

Authors:

F. Giesert[1], L. Glasl[1], A. Zimprich[1], L. Ernst[1], G. Piccoli[2], C. Stautner[1], J. Zerle[1], S.M. Hölter[1], D.M. Vogt Weisenhorn[1], W. Wurst[1,3,4,5]

Affiliations:

[1] Institute of Developmental Genetics, Helmholtz Zentrum München, German Research Center for Environmental Health, Neuherberg, Germany.

[2] Institute of Neuroscience, National Research Council, Milano, Italy

[3] Technische Universität München, Lehrstuhl für Entwicklungsgenetik, c/o Helmholtz Zentrum München, Ingolstädter Landstr. 1, 85764 Neuherberg, Germany

[4] MPI für Psychiatrie, Kraepelinstr. 2-10, 80804 München, Germany

[5] DZNE - German Center for Neurodegenerative Diseases, site Munich, Schillerstr. 44, 80336 Munich, Germany

Corresponding author:

Wolfgang Wurst
Institute of Developmental Genetics
Helmholtz Zentrum München
Ingolstädter Landstr. 1
85764 Neuherberg
Germany
Tel: +49 89 3187 4011
Fax: +49 89 3187 3099
e-mail: wurst@helmholtz-muenchen.de

Abstract:

The aim of the present study was to further explore the *in vivo* function of the *Leucine-rich repeat kinase 2* (*Lrrk2*)-gene, which is mutated in certain familial forms of Parkinson´s Disease (PD). We generated a mouse model harboring the disease-associated point mutation R1441C in the GTPase domain of the endogenous murine *Lrrk2* gene (Lrrk2-R1441C-KI line) and performed a comprehensive analysis of these animals throughout lifespan in comparison with an existing knockdown line of Lrrk2 (Lrrk2-KD line). Animals of both lines do not exhibit severe motor dysfunction or pathological signs of neurodegeneration neither at young nor old age. However, at old age the homozygous Lrrk2-R1441C-KI animals exhibit clear phenotypes related to the prodromal phase of PD such as impairments in fine motor tasks, gait, and olfaction. These phenotypes are only marginally observable in the Lrrk2-KD animals, possibly due to activation of compensatory mechanisms as suggested by *in vitro* studies of synaptic transmission. Thus, at the organismal level the Lrrk2-R1441C mutation does not emerge as a loss of function of the protein, but induces mutation specific deficits. Furthermore, judged by the phenotypes presented, the Lrrk2-R14441C-KI line is a valid preclinical model for the prodromal phase of PD.

Introduction:

Parkinson's disease (PD), as the second most common neurodegenerative disorder, is marked by the appearance of the classical clinical features like tremor at rest, rigidity of the skeletal muscles, bradykinesia and postural instability (Berardelli et al., 2001; Bloem et al., 2001; Shulman et al., 1996). These major motor-symptoms are mainly caused by the loss of dopaminergic neurons of the *Substantia Nigra pars compacta* (*SNc*) and thus can be restored by dopamine replacement therapy (Braak et al., 2004; Dickson et al., 2009). The degeneration can be accompanied by cytoplasmic protein aggregations or inclusions like *Lewy Bodies* (LBs) in various regions of the nervous system (Braak et al., 2003; Forno, 1996; Marsden, 1983; Spillantini et al., 1997). However, abnormalities of the vegetative system, neurobehavioral and sensory abnormalities can be diagnosed more than 10 years before the cardinal clinical motor symptoms caused by the loss of at least 50% to 80% of the dopaminergic neurons in the *SNc* appear (Gaenslen et al., 2011; Kordower et al., 2013). Among these preclinical features are olfactory deficits, depression and anxiety as well as sleep disorders, but also subtle motor impairments (Ebersbach et al., 1999; Siderowf and Lang, 2012). Given the fact, that this phase is the most crucial in regard to diagnosis and neuroprotective treatment of PD, it would be negligent not to invest in studying the pathoaetiology of this prodromal phase, which is indeed less studied and understood, compared to the full-blown clinical phase of the disease.

In 2004, *Leucine-Rich Repeat Kinase 2* (*LRRK2*) has been identified to be the gene responsible for PARK8-linked, autosomal dominant inherited, familial PD with classical clinical features (Funayama et al., 2002; Paisan-Ruiz et al., 2004; Zimprich et al., 2004). The LRRK2 protein harbors a variety of functional domains but most of the

pathogenic missense mutations clearly segregating with PD can be found in the enzymatic active regions of the protein like the Ras/GTPase domain (Ras of complex or Roc) or the kinase domain (Bosgraaf and Van Haastert, 2003; Giasson and Van Deerlin, 2008; Healy et al., 2008; Lesage and Brice, 2009; Paisan-Ruiz et al., 2013). Thus, there is an increasing consensus that pathogenic mutations either affect the kinase activity or the GTPase activity of LRRK2 (Nixon-Abell et al., 2016). Under certain conditions these changed activities are cytotoxic. The dominant mode of inheritance of these activity changing mutations together with - still disputed - molecular characterisations suggest that in most cases these point-mutations are gain-of-function mutations (Blanca Ramirez et al., 2016). This assumption, however, needs further investigation. The knowledge about the mode of action of the different pathogenic mutations (i.e. increasing kinase activity by the G2019S mutation and increasing GTP binding by the R1441C mutation) is of high importance in view of the fact that selective inhibition of LRRK2 kinase activity is regarded to be a promising therapeutic strategy for the treatment of PD and that lately also GTPase modifying compounds are getting center stage (Nixon-Abell et al., 2016). However, besides the analysis of changes in a single targeted molecular function (i.e. measuring autophosphorylation or GTPase activity *in vitro*), the determination of the phenotypic read-out of these mutations at the organismal level is instrumental in order to develop effective and safe LRRK2 modifying compounds. Comparing mouse models expressing the mutation in question at endogenous levels with well characterized knock-out models is a highly informative way to determine the mode of action of LRRK2.

However, so far none of the published Lrrk2 mouse lines expressing the R1441C mutation of Lrrk2 at endogenous levels show overt neurodegeneration (Liu et al., 2014; Tong et al., 2009). Minor pathological alterations like axonal swellings in tyrosine

hydroxylase(TH)-positive neurons or a hyperphosphorylation of tau protein could only be detected in transgenic rodent lines overexpressing wild-type or different mutant forms of human LRRK2 (Li et al., 2010; Li et al., 2009; Tsika et al., 2015). Unfortunately, little attention has been paid to the prodromal symptoms of PD and seldom animals >24 months of age have been analyzed. Indeed, other genetic animal models, i.e. Pink1 and DJ-1 deficient mice, when analyzed in a comprehensive and systemic manner and at these old ages, exhibit symptoms of the prodromal phase of PD (Glasl et al., 2012; Pham et al., 2010).

Thus, in order to determine the mode of action of the Lrrk2-R1441C mutation at the systemic level we have compared the cellular, pathological and prodromal behavioral characteristics of a Lrrk2 knockdown (Lrrk2-KD) mouse line based on RNA interference (RNAi)-mediated gene silencing (Delic et al., 2008) with a newly generated Lrrk2- R1441C knock-in mouse line.

Materials and Methods:

Generation of the LRRK2-R1441C mouse line

A Bacterial Artificial Chromosome (BAC) harboring the endogenous murine *Lrrk2* gene was used as a source to construct the targeting vector by means of Red®/ET® recombination. For homologous recombination a 3.9 kb long 5'-homology arm and a 6.4 kb long 3' homology arm is flanking the region around exon 31. The exon has been mutated by site-directed mutagenesis and flanked by two loxP-sites followed by a neomycin resistance cassette inserted into intron 31. $1 \cdot 10^8$ TBV2 embryonic stem cells were electroporated using 120µg linearized targeting vector with a single electric pulse for (0.1ms, 0.8kV, 3µF). Neomycin resistant clones were screened for homologous recombination by Southern blot (SB) using *BglII* (3'-probe) or *SpeI* (5'-probe) digested DNA. Correctly targeted ES cell clones were injected into C57BL/6J blastocysts and transferred into pseudopregnant CD1 foster mothers. Chimeras were bred to C57BL/6J mice and the offspring was screened for germline transmission by polymerase chain reaction (PCR) and SB analysis. The Lrrk2-KD line has been generated as described (Delic et al., 2008). Analyzed mice have been backcrossed to C57BL/6J for 3 to 5 generations in case of LRRK2-R1441C, for 5 to 7 generations in case of the Lrrk2-KD line.

Animal housing

Animal housing and handling protocols were approved by the committee for the Care and Use of Laboratory animals of the Government of Upper Bavaria (Germany) and were carried out in accordance with the European Communities' Council Directive 2010/63/EU. During the work, all efforts were made to minimize animal suffering. Wild-type mice (C57BL/6J, Charles River, Germany), as well as the LRRK2-R1441C

and knockdown lines were group housed in individually ventilated type IIL cages (maximum four mice per cage) and maintained on a 12h/12h light/dark cycle with food and water available *ad libitum*.

Genotyping assays

Genotyping was performed on genomic DNA extract from mouse tail biopsy or cell lysates both via SB analysis or PCR. For SB analysis of the 5' region of the Lrrk2-R1441C ES cell clones or mice, a radioactive labelled probe of 551bp length (amplified by the primer pairs: forward 5'-CTATTAACACCCGTGTTTGAC-3' and reverse 5'-AACAGCTCGTGTATGTTGCT-3') was hybridized to genomic DNA digested with the restriction enzyme *SpeI*. This probe labelled a 13.6kb fragment in case of the wild-type and a 5.9kb fragment of the mutated allele. For analysis of the 3' region, a probe of 486bp length (forward 5'-TGTGAGTCATGGTGACTGGTT-3', reverse 5'-GTAACAAACCCCACCCAGAA-3') was used to detect a 12.1kb fragment in case of the wild-type and a 7.5kb fragment of the mutated allele in *BglII*-digested genomic DNA. For genotyping LRRK2 R1441C animals by triplex PCR, specific primers (wild-type forward 5'-GAGAGGAATTGCCAGGACAC-3', wild-type reverse 5'-AACACAAGTCTCGGGATGAAA-3' and mutant reverse 5'-GGGGAACTTCCTGACTAGGG-3') amplified products of 626bp and 442bp length for wild-type and mutant mice, respectively. Genotyping of LRRK2 knockdown animals was performed as described previously (Delic et al., 2008).

Immunohistological and Western blot analysis

For histological analysis, animals were sacrificed and intracardially perfused with paraformaldehyde (PFA, 4%, pH 7.5). After dissection, the brain was post-fixed in PFA overnight and stored at 4°C in 25% sucrose solution until cutting in 40μm

sections. Histological methods were performed as described (http://empress.har.mrc.ac.uk/). As primary antibodies anti-LRRK2 (MJFF2, Epitomics, USA), anti-pS935 LRRK2 (Epitomics, USA), anti-Synaptophysin/P38 (#101011, Synaptic Systems, Germany), anti-Synaptotagmin 1 (#105102, Synaptic Systems, Germany), anti-alphaSynuclein mouse (Abcam, UK), anti-phosphoPHF-tau (AT8, Thermo Fisher Scientific, USA) and anti-tyrosine hydroxylase (TH) (Pel-Freez Biologicals, USA) have been used. All secondary antibodies were obtained from Jackson ImmunoResearch Laboratories (UK). For DAB (3,3' Diaminobenzidine) IHC, biotin-labeled secondary antibody (1:500; Jackson ImmunoResearch, UK) were used in combination with the Vectastain ABC System (Vector Laboratories, USA) and DAB as chromogen. Images were acquired using an Axioplan2 microscope and an AxioCam MRc camera (Carl Zeiss AG, Germany). Images were processed with AxioVision 4.6 (Carl Zeiss AG, Germany) and Adobe Photoshop CS3 (Adobe Systems Inc., USA) software. Unbiased stereology has been used to determine the total numbers of dopaminergic neurons in blinded experiments using the optical fractionator method and analyzed with the StereoInvestigator software (MicroBrightField Inc., USA). Immunopositive cells in the marked region of interest (SNc) were marked and quantified by systematic random sampling using a scan grid-size of 250x250μm.

Golgi staining of the adult CNS has been performed using the FD Rapid GolgiStain™ Kit (FD NeuroTechnologies, Inc., USA) according to the manufactures guide. After immersion, whole brains have been cryo-sectioned into 200μm sections and analyzed by 3D-reconstruction utilizing the Neurolucida software (MicroBrightField Inc., USA).

LRRK2 phosphorylation level was performed using total protein samples from adult cortex as previously described (Giesert et al., 2013) using anti-LRRK2 (MJFF2,

Epitomics, USA) and anti-pS935 LRRK2 (Epitomics, USA) as primary antibodies. HRP-conjugated secondary antibodies (Jackson ImmunoResearch, UK) were visualized using the ECL detection kit (GE Healthcare, USA).

Behavioral Analysis

Behavioral tests were applied as previously described (Hölter, S. M., and Glasl, L. (2011) in Animal Models of Movement Disorders (Dunnett, S. B. and Lane, E. eds; pp. 109–133, Humana Press, Inc., New York).

Olfaction tests

To detect graded differences in olfactory abilities, aged mice (Lrrk2-R1441C animals 24-26 months and Lrrk2-KD 24 months of age) were tested in a simultaneous smell discrimination task. The procedure was adapted from Mihalick et al. (2000) with several changes as described before (see (Glasl et al., 2012; Mihalick et al., 2000)). Odorants were presented simultaneously on fresh shavings (ratio: 1 ml per 3 g shavings) in two circular plastic dishes. For the simple condition, one dish was scented with the odorant Phenethylacetate (SIGMA, Germany; diluted to a concentration of 10 %) that was designated [S+] and the other with the same amount of solvent (Diethyl phthalate; SIGMA, Germany). The mice were trained to associate [S+] with a reward (chocolate buried in the dishes). In a more difficult condition, animals had to discriminate between [S+] and another odorant, i.e. Methyl trans-cinnamate (SIGMA, Germany; diluted to a concentration of 10 %) that was designated [S-]. Digging in the dish scented with [S+] was rewarded with chocolate. For the olfactory testing, binary mixtures of [S+] and [S-] were presented in different, increasingly similar combinations. A correct choice was defined as digging first in the dish with the higher amount of [S+] and the dish of first choice (choice accuracy in %)

was recorded. For testing smell sensitivity, binary steps of dilution were presented. A mouse responding correctly to a dish scented with [S+] was tested on the next, lower dilution step. If the animal responded incorrectly it was retested in the previous stronger step to determine the threshold.

Gait analysis

Mice with an age of 24-27 months were tested on an automated, video-based gait analysis system, the CatWalk[TM] (Noldus, Wageningen, Netherlands) as decribed before (Glasl et al., 2012). Briefly, animals ambulated over an elevated glass walkway enclosed by Plexiglas walls in a dark room. A camera (Pulnix Camera RM-765) situated below the middle of the walkway tracked the illuminated footprints, which were later analyzed with the CatWalk software Version 7.1. The software automatically calculates a wide number of parameters in several categories: (i) parameters related to individual footprints, for example, the length of a paw print; (ii) parameters related to the position of footprints, for example, stride length; (iii) parameters related to time-based relationships between footprints. For a detailed description of the Catwalk method, see Hamers et al. (2001). Data was collected without knowledge of genotype.

Vertical Pole Test

The Vertical Pole test consists of a 50 cm high, taped pole (diameter 1 cm). The animal (25-26 months of age) is placed head upward on the pole, it then orients itself downwards and descends the length of the pole to the ground. The time to turn downwards and the time to complete the task are measured. Mice received two training trials and three to five test trials with inter-trial intervals of 5 to 10 minutes.

Rotarod

Young animals (R1441C 12 weeks, Lrrk2-KD 16 weeks of age) were tested on the accelerating Rotarod (Bioseb, Letica LE 8200, Chaville, France). The rod was started with a speed of 4 rpm to allow all animals to be positioned. The speed increased to 40 rpm within 5 minutes after a trial started. Three trials were given to the animals with an inter trial interval of 15 minutes. The latency to fall was recorded.

Beam Walk and Ladder

Mice were trained to traverse a one meter long round wooden beam. After a training period, animals were placed on the beam for testing trials. The time needed to traverse the beam, the number of foot slips (both front and hind paw slips), and number of falls off the beam were measured. For the Ladder walk, animals were placed on a horizontal ladder which had variable spacing between the metal rungs. After a short training period, the mice crossed the ladder. Time needed for crossing and front as well as hind paw slips were recorded.

Open Field

Young animals (Lrrk2-R1441C 10 weeks, Lrrk2-KD 14 weeks of age) were placed in a square arena at the middle of the back wall, which is illuminated at approximately 200 lux (Actimot, TSE, Bad Homburg, Germany). For 20 minutes the behavior is recorded by the system via infra-red beam breaks.

Object Recognition

The mouse was exposed to two identical objects in an empty arena for 5 minutes. Each mouse got three sampling phases separated by 15 minutes. Three hours and 24hours after the last sampling phase one object was replaced by a new, unfamiliar

one. The exploration time of the different objects was recorded. Age at testing: 14 weeks for R1441C, 18 weeks for Lrrk2-KD animals.

Forced Swim and Tail Suspension test

The Forced Swim test was performed as described earlier (Wefers et al., 2012). Briefly, animals (Lrrk2-R1441C 8-13 weeks, Lrrk2-KD 9-16 weeks of age) were put into a 10 l beaker filled with 25 +/- 1°C water. For 6 minutes struggling, swimming and floating behavior was recorded. For the Tail Suspension test the tail of the animal was wrapped with a piece of adhesive tape and hung to a strain sensor, which recorded the activity of the animal for 6 minutes (Steru et al., 1987).

Statistical analysis

Data was analyzed using Sigma Plot 12.0 (Systat Software, Inc, Chicago, USA) and GraphPad Prism 6.0 (GraphPad Software, La Jolla, USA). Differences between two independent groups were analyzed using the t-test or the Mann-Whitney U test. For comparing more than two groups a two-way ANOVA was performed. For post hoc tests the Holm-Sidak Test was applied. For repeated measures and for the CatWalk analysis the SPSS program (SPSS Inc, Chicago, USA) was used. The chosen level of significance was $p \leq 0.05$; results with p-values between 0.05 and 0.1 were described as tendencies not reaching statistical significance.

Results:

Generation and verification of the Lrrk2-R1441C-KI mouse line

Here we present the comprehensive analysis of a Lrrk2-R1441C-KI mouse line in comparison to a previously described loss-of function model based on the ubiquitous expression of *Lrrk2*-targeting shRNA (*Lrrk2* knockdown; (Delic et al., 2008)). The Lrrk2-KD mice expressing the *Lrrk2*-targeting shRNA from one allele display an complete loss of protein in the CNS. In contrast in the adult kidney remaining LRRK2 protein - due to its extraordinary high expression, - can still be detected. Accordingly, Lrrk2-KD mice do not show a pronounced degeneration of the kidney (data not shown) as it has been reported for full KO models (Tong et al., 2010). Thus, this mouse line is very well suited to analyse the effect of loss of Lrrk2 function specifically in the CNS. In the following – if not stated otherwise – Lrrk2-KD line/mice refers to heterozygous animals in respect to the expression of the *Lrrk2*-targeting shRNA. Care was taken to compare wildtype and mutant littermates.

To generate mice expressing the endogenous murine LRRK2 with the missense point mutation R1441C in the Roc/GTPase domain, homologous recombination to "knock-in" the single nucleotide substitution c>t into the second codon of exon 31 was used. The targeting construct was generated by *Gene Bridges*© utilizing *Red*®/*ET*® recombination out of a BAC. The resulting vector consists of the 5'-homology arm of 3.9 kb length spanning the *Lrrk2* genomic region from intron 26 till 30 followed by exon 31 with the single nucleotide substitution (transition c>t) inserted by site-directed mutagenesis, flanked by two *loxP*-sites in the adjacent intronic sequences followed by a neomycin resistance cassette flanked by FRT-site and the approximately 6.4 kb long 3' homology arm which ends in intron 33 (Fig.1A,B). Mouse embryonic stem cell clones, transfected with the linearized targeting vector,

were screened by SB for homologous integration. In total three different clones have been identified and injected into blastocysts; three of the clones gave rise to in total four chimeric mice. After confirming germ line transmission by SB and sequencing (Fig.1C,D), Lrrk2-R1441C knock-in mice were crossed to a C57BL/6J background. In the following – if not stated otherwise – Lrrk2-R1441C-KI line/mice refers to animals expressing the pathogenic point mutation homozygously. Care was taken to compare for each experiment wildtype and mutant littermates.

Heterozygous and homozygous mice obtained from heterozygous brother-sister mating have been used to study possible effects of the inserted point mutation on the level and pattern of *Lrrk2* mRNA expression in the adult mouse. The expression pattern of *Lrrk2* in the brain of adult wild-type and homozygous Lrrk2-R1441C-KI mice have been studied by means of radioactive *in situ* hybridization (*ISH*). No alterations in the pattern of *Lrrk2* mRNA expression in adulthood in the CNS were found (Giesert et al., 2013) (Fig.1E). Also, no differences between wild-type and Lrrk2-R1441C-KI animals concerning the level of *Lrrk2* mRNA in the striatum as one of the most prominent expression domains of the murine *Lrrk2* gene could be detected (wild-type: 100.0% ± 1.9%; Lrrk2-R1441C-KI: 99.7% ± 4.0%) (Fig.1F).

The Lrrk2-R1441C-KI mice display no obvious initial phenotype. Heterozygote and homozygote carriers of the R1441C point mutation cannot be discriminated from their wild-type littermates in respect to size, viability and home cage behavior. Breeding heterozygote males and females, the genotypes of 3-4 week old animals are distributed according to Mendelian ratio (n=230), indicating that the mutation does not affect pre-adult stages drastically. Fertility of the mutant mice, litter size and gender distribution is also not altered.

The phosphorylation of Serine 935 has been shown to be reduced in the Lrrk2-R1441C protein (Li et al., 2011; Nichols et al., 2010). For testing the respective

phosphorylation status in the Lrrk2-R1441C knock-in mice, lysates from adult cortex were analyzed via Western blot. The quantification depicted a strong reduction in the amount of pS935-Lrrk2 normalized to the total amount of Lrrk2 protein in homozygous animals down to about 20% (Fig.1G,H). Interestingly, also heterozygous carriers of the mutation already showed a marked reduction down to 33% compared to their wild-type littermates (wild-type: 100.0 ± 12.2%; heterozygous Lrrk2-R1441C-KI: 32.5% ± 6.4%; homozygous Lrrk2-R1441C-KI: 20.3% ± 4.8%). Thus, the molecular *in vitro* characteristic of the R1441C mutation is preserved in this mouse model.

Pathological analysis

Given the highly age-related character of PD the brains of both young (5 months) and aged animals (>24 months) from the Lrrk2-R1441C-KI as well as the Lrrk2-KD line were analyzed. The second time point was chosen based on the median lifespan of the C57BL⁄6J of 866 days and 901 for females and males, respectively (Yuan et al., 2009), that is to ascertain to analyze indeed old animals. Care was taken to exclusively use "healthy" aged animals (i.e. no tumor formation). Brains were analyzed in regard to general alterations in brain morphology and in regard to pathological hallmarks of PD like dopaminergic degeneration and inclusion bodies such as Lewy bodies.

Using Nissl-staining, we could show that the gross morphology of the CNS from both mouse lines is not altered. Neither the total size, nor the size of the different brain compartments or the dimensions of the ventricles are altered in mutant animals. Also the stratification of the cortex, the folding of the cerebellar lobes and the fiber bundles innervating the brain are set up properly (data not shown). Together, these results

indicate that the general embryonic and postnatal development of the CNS remains unaltered in these animals.

To test for the pathological hallmarks of advanced PD, we first determined the number of dopaminergic neurons in both mouse lines at young and old age. The amount of dopaminergic neurons within the SNc of young Lrrk2-R1441C-KI animals was not changed (wildtype: 10221 ± 974 SEM, n=6; Lrrk2-R1441C-KI: 11052 ± 1009 SEM, n=4). Also the number of TH-positive neurons in the SNc of old animals (wildtype: 8323 ± 890 SEM, n=6; Lrrk2-R1441C-KI 6163 ± 770 SEM, n=5) was not altered between the genotype groups (Fig.2B). However, two-way Anova reveales the typical age related decline of the dopaminergic neurons in the midbrain independent of the genotype ($F_{(1, 16)}$=13,19; p=0,0022). Qualitatively and quantitatively also the innervation of the striatum, depicted by the dense network of TH-positive axonal nerve terminals, shows the same level of immunoreactivity in aged wild-type and mutant mice (wildtype: 1,000 ± 0,153 SD; Lrrk2-R1441C-KI: 1,298 ± 0,348 SD), (Fig.2C,D). To test whether the loss of Lrrk2 protein instead of the expression of mutated Lrrk2 induces dopaminergic neurodegeneration, we performed the identical analysis also for young (5 months) and aged (>24 months) Lrrk2-KD animals. And again, neither the amount of TH-positive neurons (data not shown), nor the innervation of the striatum (wildtype: 1.000 ± 0.181 SD; Lrrk2-KD: 1.047 ± 0.137 SD) (Fig.2C,D) showed impairments of embryonic or postnatal development or signs of age-related dopaminergic neurodegeneration.

Besides the loss of melanized nigral dopaminergic neurons, the occurrence of inclusions like LBs in the remaining neurons is one of the hallmarks of PD. For patients with *LRRK2*-linked PD, cases with and without LB pathology have been reported (Gaig et al., 2007; Giasson et al., 2006; Hughes et al., 2001). However, in both lines neither in forebrain regions like the olfactory bulb or cortex (data not

shown), nor in the SNc we could detect alpha-synuclein-positive inclusions (Fig.3A) or a general alteration in its expression level (Fig.3B) (wildtype: 100.0% ± 6.8% compared to Lrrk2-R1441C-KI: 98.6% ± 5.4%; wildtype: 100.0% ± 11.0% compared to Lrrk2-KD: 102.8% ± 2.9%). We also checked for the presence of *tau*-pathology as this has been reported for some cases of *LRRK2*-linked PD (Rajput et al., 2006; Ujiie et al., 2012). Again we tested aged Lrrk2-R1441C-KI and Lrrk2-KD animals but could not see distinct accumulations or a significant increase in the level of immunoreactivity in both lines (wildtype: 100.0% ± 4.9% compared to Lrrk2-R1441C-KI: 93.0% ± 3.0%; wildtype: 100.0% ± 5.2% compared to Lrrk2-KD: 99.7% ± 2.9%) (Fig.3C,D).

Altogether, the pathological analysis of Lrrk2-R1441C-KI and Lrrk2-KD animals could exclude obvious neuropathological alterations throughout the CNS. In particular, the neurons of the nigrostriatal pathway show no abnormality in regard to number, morphology or protein aggregations like synucleinopathy or tauopathy.

Morphology of the medium spiny neurons in the striatum of the Lrrk2-R1441C-KI and Lrrk2-KD line

It has already been shown, that primary hippocampal neurons prepared from newborn knockdown animals exhibit a slight increase in neurite branching (MacLeod et al., 2006). Thus, we analysed the dopaminoceptive neurons of the striatum - the medium spiny neurons (MSN) - which comprise the majority of neurons of this main input nucleus of the dopaminergic projectins (Tepper and Bolam, 2004) and show the highest neuronal expression of Lrrk2 (Galter et al., 2006; Giesert et al., 2013; Melrose et al., 2006; Simon-Sanchez et al., 2006). For this, brains of adult Lrrk2-R1441C-KI and Lrrk2-KD mice and their corresponding wildtype littermates were stained using the classical technique of Golgi (Fig.4A,B). The morphology of Lrrk2-

R1441C-KI MSNs was very similar to control neurons as revealed by quantitative analysis using a 3D-reconstruction program (Neurolucida; Fig.4C, E, G). Also the analysis of Lrrk2-KD animals did not reveal significant differences. However, it has to be mentioned, that in this line all primary parameters like neurite quantity (wildtype: 24.19 ± 1.69; Lrrk2-KD: 30.44 ± 3.67) or overall neurite length (wildtype: 1508µm ± 447; Lrrk2-KD: 2031µm ± 621) were always, albeit not significantly, increased (Fig.4D). Sholl analysis of the dendritic arbor also showed a consistent trend (p=0.16) for increased arborisation particularly in a region about 30µm around the neuron, which, however, again did not reach significance (Fig.4F). Taken together, Lrrk2-R1441C-KI neurons do not show morphological alterations at the postsynaptic side of the nigrostriatal pathway, whereas Lrrk2-KD neurons exhibit subtle trends towards an increase in branching and network complexity.

Synaptic transmission

On the functional level, the loss of Lrrk2 or the expression of mutated forms of Lrrk2 can induce alterations of synaptic transmission, both in dopaminergic and glutamatergic neurons (Melrose et al., 2010; Piccoli et al., 2011; Tong et al., 2009). Based on this, we studied the process of synaptic vesicle exocytosis- and endocytosis-events in primary cortical neurons, prepared from single Lrrk2-R1441C-KI or Lrrk2-KD embryos and their wildtype littermates. In parallel, we analyzed the effect of an acute knockdown approach using lentiviral mediated infection of primary neurons obtained from wild-type C57BL/6J with a siRNA directed against Lrrk2 published before (Piccoli et al., 2011).

The basal exo-/endocytosis rate in Lrrk2-R1441C-KI neurons of 34% (±2.5) was comparable to wildtype neurons (32% ± 3.4). The evoked activity in a depolarizing high-potassium buffer (supplemented with 50mM KCl) was enhanced in both

genotypes to a similar degree (wildtype neurons: 39% ± 2.2%; Lrrk2-R1441C-KI neurons: 43% ± 4.3%) (Fig.5C). The ratio of synaptotagmin-positive vesicles to the total number of vesicles in wild-type controls was comparable between the different control groups and fits to the range of published data using a comparable loading time (Bacci et al., 2001). Interestingly, testing neurons prepared from Lrrk2-KD mice revealed that the constitutive loss of Lrrk2 protein only leads to a slight but non-significant (p=0.29) increase of vesicle turnover rate from 34.17% (± 4.15%) in wildtype controls to 38.23% (± 2.67%) in Lrrk2-KD neurons (Fig.5B). In contrast, the acutely Lrrk22-depleted neurons did show a significant (p<0.01) increase of nearly two fold in their basal synaptic vesicle turnover rate from 34.17% (±4.15%) in non-treated to 55.87% (±6.21%) in viral infected neurons (Fig.5B and (Piccoli et al., 2011)).

These results strongly suggest that alterations in the dynamics of exo-endocytosis are compensated in constitutive Lrrk2-KD neurons, whereas the phenotype is obvious under acute knock-down conditions.

Behavioral analysis of Lrrk2-R1441C and knockdown mice

Motor symptoms

We subjected both lines to commonly used motor tests, amongst which are the Open Field, Rotarod and Grip Strength. An initial analysis of Open Field data, gathered in young animals at the age of 10 weeks and of data gathered from the Rotarod test at the age of 12 weeks, did not reveal any differences with regard to locomotion and coordination, respectively, in both mouse lines.

However, since PD is a progressive age related disorder, we analysed both mouse lines also at older ages for locomotor behavior. In order to detect subtle changes in

locomotion we choose more sophisticated tests such as the Ladder - and Beam Walk test, as well as the Vertical Pole test, which is reported to be indicative for disturbances in the nigrostriatal system (Matsuura et al., 1997; Ogawa et al., 1985). Indeed, in mice older than 24 months we saw subtle changes when subjected to the Ladder and Beam Walk test. These changes, however, were only detectable in the Lrrk2-R1441C-KI line, not in the knock-down (Lrrk2-R1441C-KI: Beam: increased total slips: p= 0.016; U= 0.000; Median: wildtype: 6.5, Lrrk2-R1441C-KI: 12.0; Ladder: increased time p= 0.052; U= 4.5; Median: wildtype: 15.5, Lrrk2-R1441C-KI: 20.0, and slips p= 0.082; U= 5.0; Median: wildtype: 2.0, Lrrk2-R1441C-KI: 4.0) (see Fig. 7B). Similar results were obtained while applying the Vertical pole test. Lrrk2-R1441C-KI animals took longer than their controls to turn and to complete the trial (Time to turn: U= 4.0, p= 0.03, Median: wildtype: 4.5, Lrrk2-R1441C-KI: 10.75, see Fig. 7A; Time to complete: U=5.0, p=0.048, Median: wildtype: 9.75, Lrrk2-R1441C-KI: 26.25). There was a tendency for an increased time to descend (Time to descend: U=6.0, p= 0.073, Median: wildtype: 5.25, Lrrk2-R1441C-KI: 15.5). Again for the Lrrk2-KD animals no such differences were found.

In order to exclude any effect of muscle strength on these behaviors, we also performed the Grip Strength test at this old age, which did not reveal any differences in either mouse line (data not shown). Thus, in respect to Lrrk2 function, the loss- and putative gain-of-function mouse models differ in their motoric behavior at old ages.

Gait

Since we had indications that subtle motoric phenotypes are present at old ages, we further elucidated this phenotype by a gait analysis. We used the CatWalk® system to detect changes in gait, analyzing both temporal and static parameters. The angle at

which the front paws were placed was significantly different in the Lrrk2-R1441C-KI animals ($F_{(1,11)}$=8.395; p=0.02), and additionally a trend towards changes in the coupling of the left hind to right front paw ($F_{(1,11)}$=4.161; p=0.076) was detected, pointing towards diminished paw coordination in mutant animals (Fig. 7C,D).

In the Lrrk2-KD mouse line clear sex-genotype interactions occurred (Fig. 8). The print length ($F_{(1,39)}$=5.913, p= 0.02; males: p=0.04, females: ns), the swing speed ($F_{(1,39)}$=7.183, p= 0.011; males: p= 0.06, females: ns) and the stride length ($F_{(1,39)}$=7.144 , p= 0.011; males: p= 0.076, females: p=0.049) of the front paws showed all a significant sex-genotype interaction, with the male mutants showing a reduction in all three parameters and female mutants showing an increase in stride length compared to their respective controls. The maximum contact at (%), the point where the braking phase of a step turns into the propulsion phase, was significantly increased in the male mutants ($F_{(1,39)}$=7.278, p= 0.011; males: p= 0.009, females: ns). Also impairments in paw coordination were observed (Phase Dispersion Diagonal: $F_{(1,39)}$=4.246 , p= 0.047; males: p= 0.028, females: ns).

Taken together, the gait analysis in old animals at the age of 24-27 months revealed gait disturbances in both lines. These changes were related to parameters associated with paw placement and leg coordination.

Analysis of symptoms of the prodromal phase of PD

Since the above behavioral analysis indicated that at least in the R1441C knock-in mouse line disease aetiology is ongoing we further analyzed the lines for phenotypes known to occur in the prodromal phase and/or being established as comorbide symptoms, such as cognition deficits, olfactory dysfunction and anxiety and depression-like behavior. Due to the fact that locomotor dysfunction was only detectable at older ages, we hypothesized that the likelihood to detect these

symptoms is increased at older age. Whereas animals of both lines did not depict any deficiencies in the cognition as evaluated by the object recognition test (data not shown) phenotypes concerning olfactory function and anxiety and depression-like behavior could be detected.

Olfactory function

Hyposmia is one of the most widespread non-motor symptoms occurring very early in the course of the disease and it is actually already used for prediction and diagnosis of PD (for review see (Haehner et al., 2009)). Based on this, we utilized an odor discrimination paradigm to test for olfactory abilities. To test for sensitivity mice had to detect an assigned odor with increasing dilutions. For discrimination abilities they had to discriminate between binary mixtures of two different odors (Glasl et al., 2012). In the Lrrk2-R1441C-KI line a significant reduction in odor sensitivity was detected (U=18; p=0.014). Also in the discrimination task the Lrrk2-R1441C-KI mutants performed worse than the wild-types ($F_{(1,17)}$=5.685; p=0.029) (Fig.6A,B). Similar deficits were seen also in the Lrrk2-KD animals, albeit not to the same extent. While males showed a trend towards a deficit in odor sensitivity (U= 23.5; p=0.056), the deficits in females were more pronounced and found to be significant (t_{10}=2.7, p= 0.022) (Fig.6C,E). In the discrimination task no differences between genotypes in the Lrrk2-KD animals could be observed (Fig.6D,F).

Anxiety related and stress-coping behavior

In order to assess anxiety-related behavior we first analyzed the Open Field parameters related with this behavior at young age (10-14 weeks). While Lrrk2-R1441C-KI animals did not show significant changes in that respect (Fig. S1A), mice of the Lrrk2-KD line spent significantly more time in the center of the test arena

($F_{(1,45)}$= 4.747, p= 0.035) (Fig. S2A). According to the Open Field exposure paradigm (Prut and Belzung, 2003), this behavior can be interpreted as a reduction in anxiety-related behavior. Thus, to further evaluate alterations in emotional behavior, the Forced Swim and the Tail Suspension test were performed (Cryan et al., 2005; Trullas et al., 1989). Again, in order to detect more pronounced effects we decided to test at older ages (from 8-15 months, thus mid-aged animals). In the Forced Swim test Lrrk2-R1441C-KI mice showed a significant decrease in time spent floating already at the age of 9,5 months ($F_{(1,40)}$= 6.895, p= 0.012) (Fig. S1B). In contrast, in Lrrk2-KD animals no significant changes could be observed, even at the age of 15 months (Fig. S2B).

Parameters of the Tail Suspension test were significantly altered in both lines. In the Lrrk2-R1441C-KI line at the age of 8 months, the females showed an increased latency to immobility (trend in sex-genotype interaction: $F_{(1,42)}$= 3.698, p= 0.062; Genotype effect: $F_{(1,42)}$= 5.864, p= 0.02; Holm Sidak Test: males: ns, females: p= 0.005) (Fig. S1C and D). At the age of 12 months Lrrk2-KD animals of both sexes showed a significant ($F_{(1,51)}$= 8.082, p= 0.007) reduction in the mean duration of immobility (Fig. S2D), as well as a trend in the total duration of immobility ($F_{(1,51)}$: 3.506, p= 0.067) (Fig. S2C). Taken together, animals of both lines show reduced depression-like behaviors. In addition the Lrrk2-KD line exhibited reduced anxiety-related behavior as indicated by the Open Field data.

In summary (Table 1), both lines do not recapitulate the pathological hallmarks of PD or show morphological changes in the nigrostriatal system. Nevertheless, on the behavioral level, both Lrrk2 lines depict phenotypes. The Lrrk2-KD line is conspicuous for its phenotypes related to depression-like behavior. The Lrrk2-R1441C-KI line exhibits more robust behavioral phenotypes with respect to

prodromal symptoms (olfaction, gait) as well as clear cut impairments in tests for subtle motoric phenotypes at old ages.

Discussion:

To shed light on the functional role of LRRK2 itself and one of its pathological point mutations in PD etiology (R1441C), this systematic and comprehensive study is comparing two different Lrrk2 mouse lines: a line with a constitutive knock-down of Lrrk2 (Lrrk2-KD; (Delic et al., 2008)) and a line with a knock-in of the pathogenic point mutation R1441C of Lrrk2 (Lrrk2-R1441C-KI). The analysis was performed on the neuropathological, molecular and behavioral level throughout lifespan and the results discussed below are summarized in Table 1.

Generation of the Lrrk2-R1441C-KI mouse line

The newly generated Lrrk2-R1441C-KI mouse line was generated by knocking in the c>t transition into the endogenous murine *Lrrk2* locus, giving rise to the pathogenic point mutation R1441C on the protein level. Thus, this mouse line mimics the genetic composition of patients, i.e. the R1441C point mutation. In addition, in future studies this mouse line will be highly suitable to dissect the role of the Lrrk2 GTPase domain *in vivo,* since the floxed exon 31 – encoding for the 73 amino-acid long C-terminal part of the Roc-GTPase domain – can be deleted using a Cre-driver line. This deletion will disrupt the Roc-GTPase domain of Lrrk2, leaving, however, its kinase domain intact.

To rule out that observed phenotypes are due to changes in Lrrk2 expression levels induced by the point mutation in this model, we performed a thorough analysis of *Lrrk2* mRNA expression. No alterations in regard to expression level and pattern, both in young and aged animals of this line were detected. Additionally, also the expression of the *Lrrk2*-paralog *Lrrk1* was not changed in the Lrrk2-R1441C-KI line

(data not shown). Thus, the phenotypes described for this model are attributable to an effect of the single point mutation.

We further confirmed the functionality of the knock-in model on a molecular level by studying the constitutive phosphorylation site Serine 935 (Dzamko et al., 2010; Gloeckner et al., 2010; Li et al., 2011; Nichols et al., 2010) in brain lysates from adult animals. Mice homozygous for the R1441C Lrrk2 point mutation did show a marked reduction of phosphorylation down to 20.3% at that site, resembling previous results from BAC transgenic mice (Li et al., 2011). The fact, that 50% of remaining wildtype protein in heterozygous animals is not sufficient to keep up at least half of the constitutive phosphorylation level might be due to changes in Lrrk2 dimerization, differential activity of upstream kinases/phosphatases, and/or differential regulation of Lrrk2 kinase activity by the binding of 14-3-3 protein (Ito et al., 2014; Lobbestael et al., 2013; Muda et al., 2014; Reynolds et al., 2014). Given the fact that phosphorylation of S935 and 14-3-3 protein binding is involved in the subcellular redistribution of the protein (Deng et al., 2011; Dzamko et al., 2010; Mamais et al., 2014), one can hypothesize that like in Lrrk2-KD cells, also in Lrrk2-R1441C-KI cells, Lrrk2 is not present at its distinct activity areas, which might result in a loss-of-function phenotype.

Pathological analysis

The analysis of the dopaminergic system in young Lrrk2-R1441C-KI and Lrrk2-KD animals did not reveal qualitative or quantitative changes neither at young nor old ages (up to 28 months of age). Further PD associated pathologies such as the formation of LBs, Lewy neurites, up-regulation of alpha-synuclein and neurofibrillary tangles or Tau-pathology in young and old mice of both lines were also not detectable *in vivo*. Neurite morphology was also not changed in both lines. These

findings confirm the results of previously published Lrrk2 mouse models based either on a knock-in of R1441C into the endogenous murine *Lrrk2* gene or the full knockout of the gene (Tong et al., 2009; Tong et al., 2010). They, however, seem to contrast earlier studies in which disturbances in Lrrk2 biology induce substantial dopaminergic neurodegeneration and hyperphosphorylation of Tau and AT8-positive neurites. This difference, however, might be due to the overexpression of LRRK2 or mutated LRRK2 in the BAC transgenic mice at very high levels, which by itself might induce cellular toxicity and/or might surpass existing compensatory mechanisms. In favor of compensatory mechanisms in place is the fact, that in contrast to *in vitro* analysis (Lavalley et al., 2016), neuritic morphology of MSNs of both lines is not significantly changed, even though the MSNs in Lrrk2-KD animals exhibit a non-significant trend towards an increase in nearly all evaluated parameters. No detectable impairments in exo-/endocytosis processes in primary neurons, neither from the Lrrk2-R1441C-KI mice nor from constitutive Lrrk2-KD - contrasting the results from acute knock-down - also speak in favor of compensatory processes. Differences to results in primary cortical tissues from G2019S knock-in animals and/or striatal brain slices might again be attributed to high levels of overexpression, or in this case also to different mutations or different experimental methods and culture systems applied (Beccano-Kelly et al., 2014a; Beccano-Kelly et al., 2014b; Chou et al., 2014; Parisiadou et al., 2014).

Behavioral analysis

The pathological findings, specifically the absence of overt degeneration of dopaminergic neurons, are corroborated by the behavioral analysis, since in both lines no severe motor changes were observed. This finding has also been reported by others independent of the genetic make-up of the respective mouse lines (Andres-

Mateos et al., 2009; Bichler et al., 2013; Hinkle et al., 2012; Liu et al., 2014; Tagliaferro et al., 2015; Tong et al., 2009; Tong et al., 2010; Volta et al., 2015; Weng et al., 2016). However, subtle motoric dysfunctions have been reported in the transgenic R1441G line (Dranka et al., 2013; Dranka et al., 2014), a finding which is confirmed by this study in old animals expressing the pathogenic form at endogenous levels. Thus, the dopaminergic system might be functionally impaired in old Lrrk2-R1441C-KI animals, even though no degeneration of the dopaminergic neurons was detectable. However, in these old mice dopamine release or the sensitivity of MSNs expressing Lrrk2 at very high levels might be altered resulting in fine motoric symptoms. Interestingly this phenotype is not observed in aged Lrrk2-KD animals, which is again in agreement with former studies (Andres-Mateos et al., 2009; Hinkle et al., 2012; Tong et al., 2010; Volta et al., 2015). Thus, the dysfunction in these fine motor tasks in the Lrrk2-R1441C-KI line are highly likely attributable to altered Lrrk2 function due to the pathogenic point mutation rather than a general loss of function of the protein in the brain. This is in agreement with the notion that the R1441C mutation is thought to be a gain-of-function mutation rather than a loss-of-function mutation. It has been reported, that in humans fine motor capabilities are impaired in patients about 3-4 years prior to the definitive PD diagnosis (Noyce et al., 2016; Postuma et al., 2012), which might be regarded as symptoms of the prodromal phase of the disease.

Interestingly, the Lrrk2-R1441C-KI line also exhibits further symptoms of the prodromal phase such as gait alterations. Gait alterations are already detectable in asymptomatic carriers of the mutation and the ones observed in the Lrrk2-R1441C-KI mouse line are reminiscent to the ones in PD patients, i.e. affecting coordination (Baltadjieva et al., 2006; Mirelman et al., 2011; Shulman et al., 1996). Gait phenotypes are also observed in the Lrrk2–KD line – albeit less robust. This indicates

that a functional Lrrk2 protein – independent of the pathogenic point mutation – is necessary to execute proper gait control. Neuronal circuits implemented in gait control extend beyond the dopaminergic system and involve also the cholinergic and serotonergic brainstem, especially the nucleus pedunculopontinus, and the spinal cord (Alam et al., 2011). All of these regions are known to express Lrrk2 (Giesert et al., 2013). It would be interesting to evaluate the contribution of these neuronal systems towards the gait phenotype by using appropriate conditional mouse models.

In addition, the Lrrk2-R1441C-KI line presents a further prodromal symptom: the olfactory dysfunction. In contrast to our findings, Bichler et al. reported no alterations of olfaction in animals overexpressing a R1441G mutation (Bichler et al., 2013), but using the same mouse line as Bichler et al., another report describes an hyposmic phenotype (Dranka et al., 2014). Since we only detected alterations in fine tuning of olfaction such as sensitivity and discrimination these animals are not impaired in smelling per se. Also PD is not characterized by the complete loss of smelling but rather by loss of sensitivity and discrimination capabilities (Haehner et al., 2014). Specifically in Lrrk2 mutation carriers the olfactory phenotype is less benign than in idiopathic PD fitting to our subtle but clear phenotype(s) (Ruiz-Martinez et al., 2011; Saunders-Pullman et al., 2014). Compared to Lrrk2-R1441C-KI mice Lrrk2-KD mice show a weak phenotype: only males are impaired in the sensitivity task and no phenotype is observed in the discrimination task in neither sex. Thus, like for the fine motor tasks, the loss of Lrrk2 function seems not to be the underlying cause of the symptom, rather the specific pathogenic point mutation.

Another prodromal symptom, depression, has also been reported in PD. However, in Lrrk2 mutation carriers - specifically R1441C/G carriers - this seems to be a rather infrequent symptom (Bergareche et al., 2016). In contrast to the human situation, the Lrrk2-R1441C-KI line shows reduced depression-like behavior. In this respect, the

Lrrk2-KD mice exhibit reduced anxiety-related behavior as indicated by the Open Field data, which is in contrast to the reported thigmotactic behavior of Lrrk2 knock-out animals (Hinkle et al., 2012). The latter difference might be explainable by differences in genetic background of the mouse lines examined or the different experimental settings being used. The reason for this discrepancy between human and mouse is not readily explainable but might relate to the complexity of the neuronal circuits underlying depressive behavior and compensatory mechanisms in place.

Preclinical models for PD?

Taken together the analysis of our mouse lines reveals that specifically the Lrrk2-R1441C-KI line recapitulates the prodromal phase of PD but does not progress to the full phenotype, i.e. the degeneration of the dopaminergic neurons, of the disease. In addition, literature in respect to reported phenotypes of genetic mouse models of PD is not homogenous. Thus, a discussion of these two points – independent of the single mouse lines presented here – is warranted.

The first and easiest explanation for the weak phenotype of the genetic PD mouse models might be the existence of fundamental species differences. However, the growing literature in the iPSC field does not yet indicate a fundamental difference concerning molecular function and/or cellular phenotypes (own unpublished data). Another attractive hypothesis is the short lifespan of mice as compared to humans and thus a reduced accumulation of potential hazardous environmental impacts to which Lrrk2 mutation carriers seem to be more susceptible. This short lifespan, however, also might implicate that in mice compensatory mechanisms are still in

place, which might be overcome by premature ageing (Miller et al., 2013). The existence of potential compensatory mechanisms in mice has already been discussed due to the observed discrepancy of *in vitro* models, implementing an acute knock-out versus *in vitro* models derived directly from the mouse line in question ((Glasl et al., 2012)). These compensatory mechanism might be manifold, but might also include the activation of molecular protective mechanisms not directly related to the function of the protein in question, per se (Pham et al., 2010). Thus, to fully understand the function of a protein and/or pathogenic mutations, it is not sufficient to analyze acute phenotypes *in vitro.* However, and specifically in the case of complex diseases, it is of utmost importance to also take into account the systemic aspect – that is the whole organism. In the long run such a notion could induce a shift from focusing on repairing disease causing mechanisms to increasing protective mechanisms as potential therapeutic targets.

Concerning the lack of the major symptoms of PD in Lrrk2 mouse models also the multifactorial nature of the disease has to be taken into account. Strong motor deficits, accompanied by severe dopaminergic degeneration have been observed up to now only in toxin-induced lesion models of PD (Byler et al., 2009), whose effect can be modulated by genetic factors. In Lrrk2 mouse models alterations in motor features appear to depend on an environmental challenge, e.g. a reduced inhibition of locomotor activity by quinpirole in Lrrk2-R1441C-KI mice (Tong et al., 2009). These findings are in agreement with the hypothesis of the multifactorial nature of PD (Farrer, 2006), requiring an interaction and additive of different pathoetiological factors such as genetic predisposition (given in these mouse models) and exposure to environmental detrimental factors (not applied in our study).

The also troublesome fact of inconsistency concerning phenotypes of genetic mouse models of PD reported in literature, is exemplified by the finding, that the results of the present Lrrk2-R1441C-KI line seem to be in sharp contrast to the original publication of a mouse line expressing a transgene with a highly similar R1441G mutation. The latter exhibits a 5-10 fold higher expression level of the pathogenic mutation and is kept on a FVB/NJ genetic background (Bichler et al., 2013; Li et al., 2009; Tagliaferro et al., 2015; Weng et al., 2016). This - at a first glance - inconsistency between the different reports feeds well into the recent debate about irreproducibility of phenotypes in animal models, questioning them as being good predictive preclinical models (Begley and Ioannidis, 2015; Frye et al., 2015; Steckler, 2015). However, by taking a closer look, these inconsistent results strongly suggest, that there exists a non-neglectable dependency of the phenotype on the genetic design as well as the genetic background. This should not be too surprising when taking into account, that there also exist non-manifesting human mutation carriers of the R1441C/G mutation (even though they have to be regarded as being "at high risk to develop the disease") (Pont-Sunyer et al., 2015). These circumstances clearly call for standardization of animal models, assays (specifically behavioral assays) and statistically sound numbers of animals throughout the scientific community, to be able to compare results of animal models specifically of common, multifactorial diseases, which often do "only" display subtle phenotypes in the range of 10-20% differences (Wurst, 2016).

Conclusions

Taken together, our comparative analysis of the Lrrk2-R1441C-KI mice with the Lrrk2-KD mice reveals three major insights.

1. Due to the different phenotypes induced by the knock-down of Lrrk2 as compared to the phenotypes induced by the expression of its pathogenic mutation R1441C it can be concluded, that the effect of the pathogenic mutation is not based on the loss of function of Lrrk2. Rather it is a mutation specific effect, which might open up new therapeutic avenues beyond the inhibition of the Lrrk2 kinase activity (Nixon-Abell et al., 2016).

2. The Lrrk2-KD mouse line reveals that Lrrk2 is involved in molecular mechanisms which have been implicated in the pathoetiology of PD (i.e. impaired neurotransmitter release). Thus it is a valid model to study the function of Lrrk2 in PD associated neuronal systems.

3. The Lrrk2-R1441C-KI line presents with the symptoms highly reminiscent of the prodromal / early phase of PD in humans, carrying this specific *LRRK2* mutation. Thus, it represents a valid preclinical model to study the pathoetiology of prodromal PD *in vivo.*

Acknowledgements:
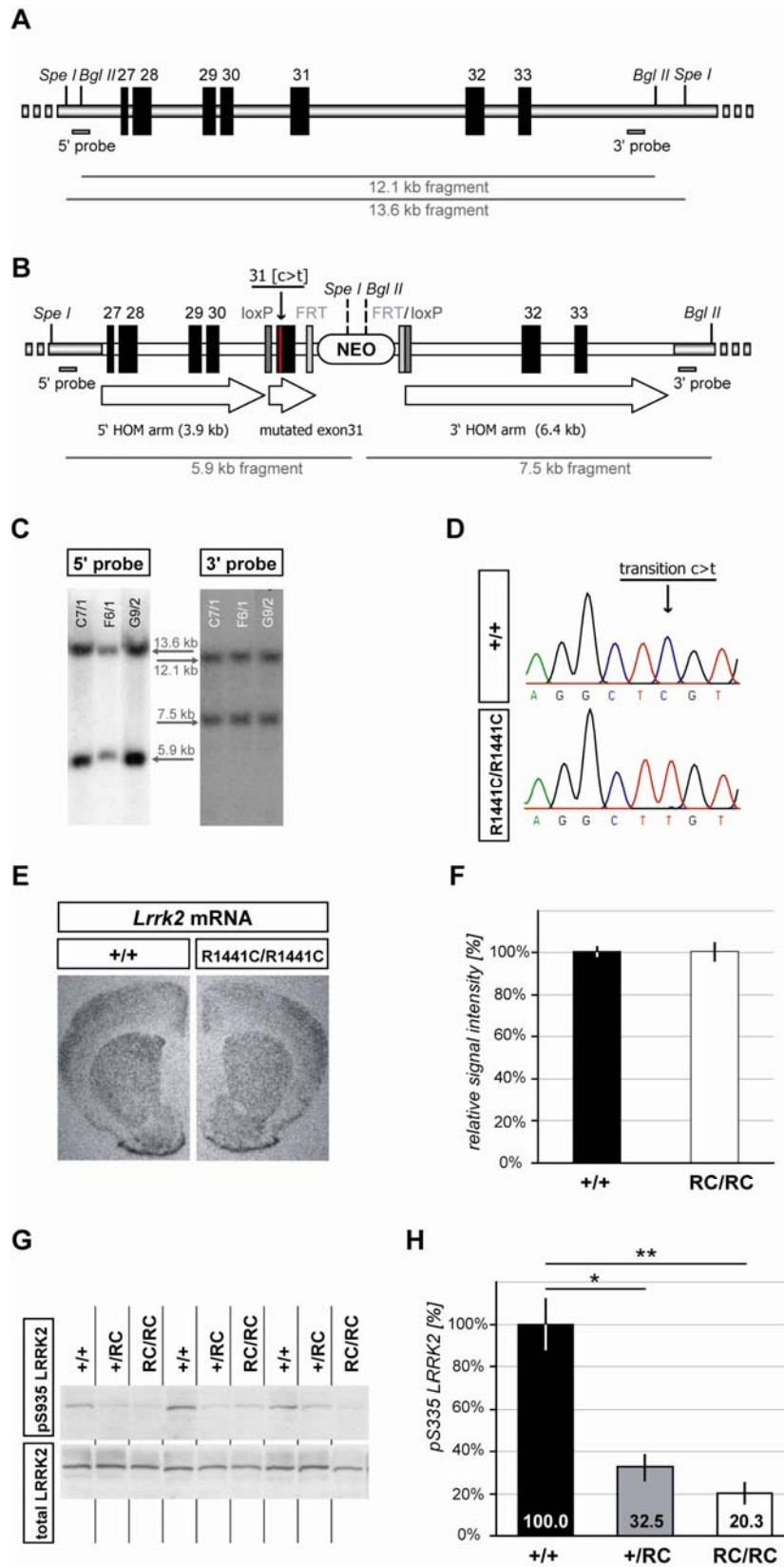
Figures/Figure Legends:

Figure 1: **The Lrrk2-R1441C-KI line expresses _Lrrk2_ mRNA on endogenous pattern and level, but Lrrk2-R1441C protein is hypophosphorylated on Serin-935. A,B**) The targeting strategy is based on the homologous recombination of the point-mutated _loxP_-flanked exon 31, followed by a selection marker into the endogenous _Lrrk2_ locus. Part of the endogenous genomic _Lrrk2_ locus with its exons 27-33; the genomic locus after integration of the targeting construct (red) consisting of the 5'- and 3'-homology arm (HOM arm), the _loxP_-flanked exon 31 bearing the transition c>t, followed by the _FRT_-flanked neomycin resistance cassette. The wild-type and mutated mRNA and protein sequences indicating the resultant missense mutation R1441C. **C**) Verification of the correct targeting in Lrrk2-R1441C embryonic stem cell clones by Southern blotting using 5'- and 3'-probes. **D**) Verification of the inserted c>t transition in the first position of the second codon of exon 31 from wild-type and homozygous Lrrk2-R1441C-KI mice by sequencing. **E,F**) The expression level and pattern is not changed in homozygous Lrrk2-R1441C-KI mice: coronal forebrain section showing the identical _Lrrk2_ mRNA expression by in situ hybridization (ISH) (left). Quantification of the ISH signal in the striatum indicates that _Lrrk2_ mRNA levels remain unaltered in the brain of homozygous Lrrk2-R1441C-KI mice compared with their wildtype littermates up to an age of 24 months (n=2/2) (right). **G,H**) The amount of LRRK2 phosphorylated on serine 935 (pS935 LRRK2) normalized to the level of total LRRK2 protein is reduced (wildtype: 100.0 ± 12.2%; Lrrk2-R1441C-KI heterozygote: 32.5% ± 6.4%; Lrrk2-R1441C-KI homozygote: 20.3% ± 4.8%), both, in heterozygous (p=0.016, Student's t-test) as well as homozygous (p=0.008, Student's t-test) carriers of the R1441C mutation (G, representative Western blot; H quantification; n=5) (Graphs represent the mean with standard error).
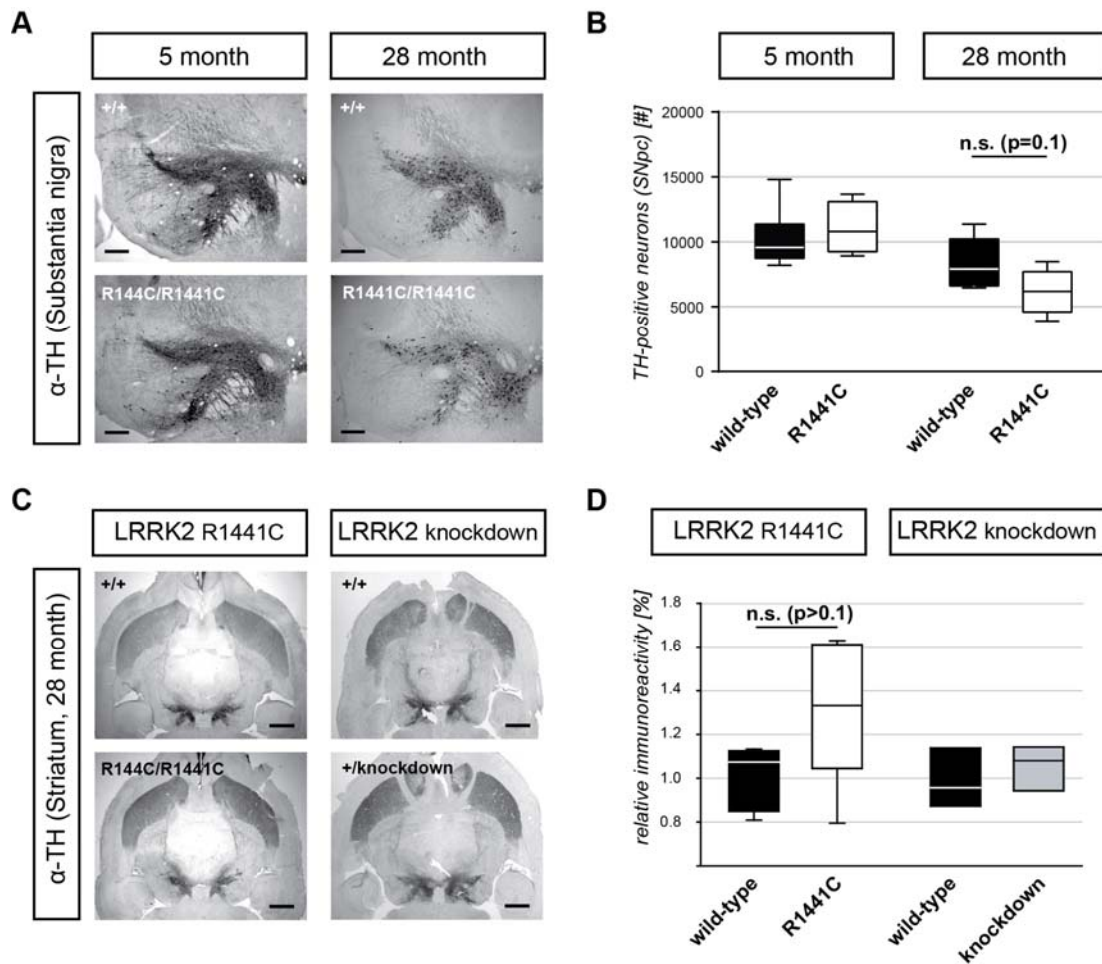
Figure 2: **Lrrk2-R1441C-KI and Lrrk2-KD animals do not exhibit dopaminergic degeneration.** **A**) Representative pictures from DAB-Immunohistochemistry for *Tyrosine Hydroxylase* (TH) on horizontal midbrain sections of young (5 months) and aged (28 months) Lrrk2-R1441C-KI animals (lateral on left, rostral on top) illustrating the substantia nigra. **B**) B) Quantification of dopaminergic neurons in young and aged Lrrk2-R1441C-KI animals (5 months: 10221 ± 974 SEM in wildtype to 11052 ± 1009 SEM in mutant; 28 months: 8323 ± 890 SEM in wildtype to 6163 ± 770 SEM in mutant). **C**) Representative pictures from DAB-Immunohistochemistry for *Tyrosine Hydroxylase* (TH) on horizontal sections of aged (28 months) Lrrk2-R1441C-KI and Lrrk2-KD animals in forebrain and midbrain (lateral on left, rostral on top), illustrating

the nigrostriatal innervation. **D**) Quantification of the dopaminergic innervation in the aged striatum (Lrrk2-R1441C-KI: 1,000 ± 0,153 to 1,298 ± 0,348; Lrrk2-KD: 1.000 ± 0.181 to 1.047 ± 0.137). Number of animals: 5/5 (wt/mut). Scale bars represent 1000 µm (A) and 250 µm (C) (Box plots represent the 10th, 25th, 75th and 90th percentile with the median).
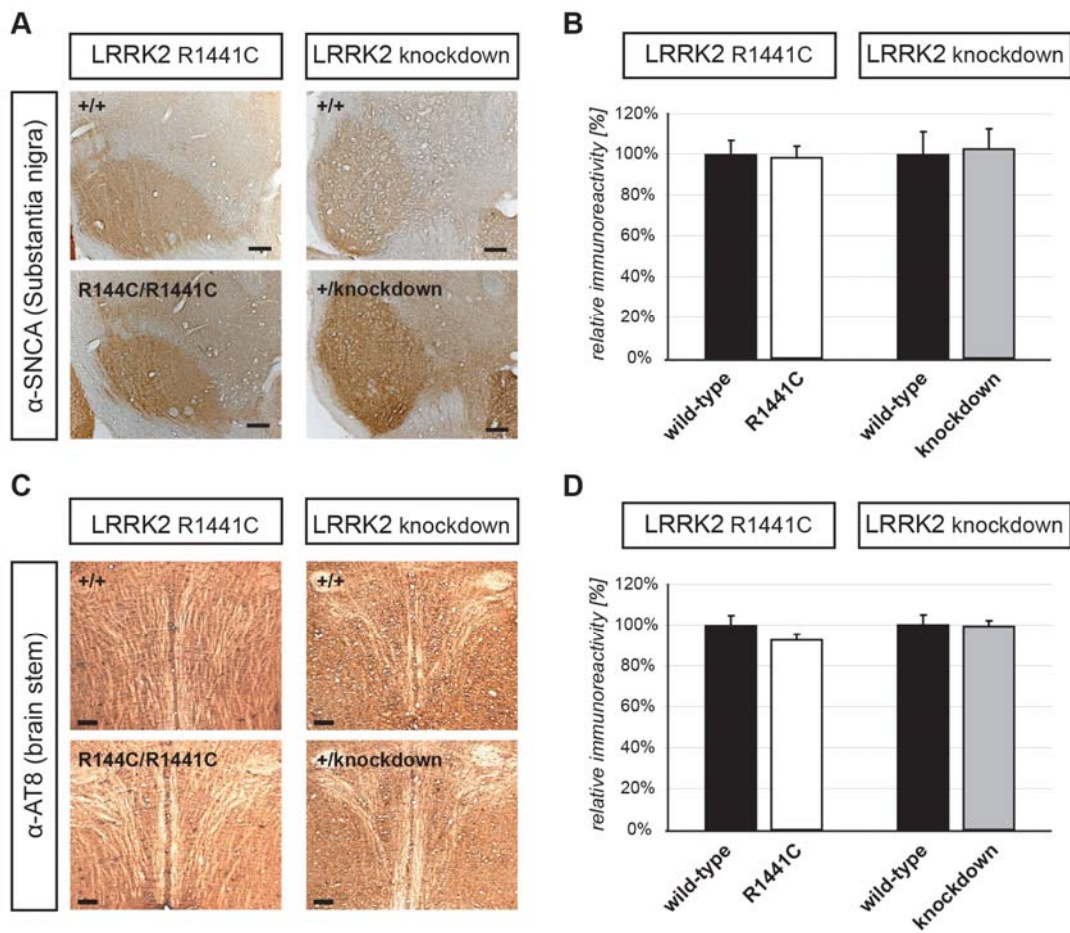
Figure 3: **Lrrk2-R1441C-KI and Lrrk2-KD animals do not show PD-related pathology. A**) Representative pictures from DAB-Immunohistochemistry for alpha-Synuclein (SNCA) on horizontal sections of aged (28 months) Lrrk2-R1441C-KI and Lrrk2-KD animals of the ventral midbrain (lateral on left, rostral on top), illustrating the absence of alpha-synuclein (SNCA) positive inclusions in the aged brain of both models. **B**) Quantification of the relative immunoreactivity in the *Substantia nigra pars compacta* and *reticulata* revealed comparable levels of SNCA expression in these regions both in Lrrk2-R1441C-KI and Lrrk2-KD animals (Lrrk2-R1441C-KI: 1.00 ± 0.07 in wildtype to 0.99 ± 0.05 in mutant; Lrrk2-KD: 1.00 ± 0.11 in wildtype to 1.03 ± 0.10 in mutant). **C**) Representative pictures from DAB-Immunohistochemistry, using the AT-8 antibody detecting *Paired helical filaments* marked by hyperphosphorylated

Tau protein in horizontal sections of the hindbrain on the level of the *medial longitudinal fasciculus*. Aged Lrrk2-R1441C-KI and Lrrk2-KD animals do not show signs of tau-pathologies throughout the brain. **D**) Quantification of the relative immunoreactivity in the brain stem of Lrrk2-R1441C-KI and Lrrk2-KD animals supports this finding (Lrrk2-R1441C-KI: 1.00 ± 0.05 in wildtype to 0.93 ± 0.05 in mutant; Lrrk2-KD: 1.00 ± 0.03 in wild-type to 0.99 ± 0.03 in mutant) (Graphs represent the mean with standard error).
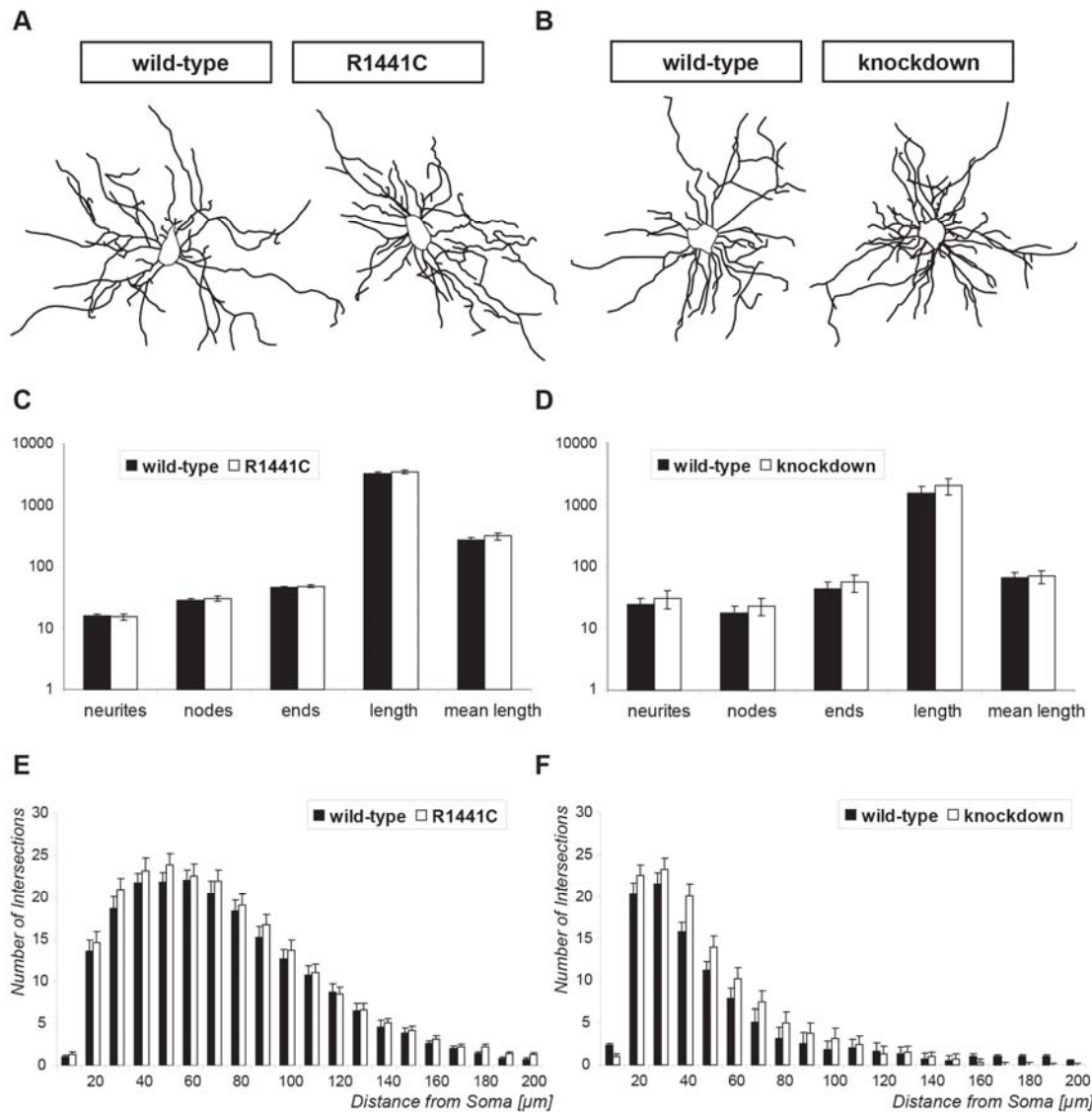
Figure 4: **The morphology of the dopaminoceptive striatal medium spiny neurons is not altered in both mouse lines. A**,**B**) Representative projections of 3D-reconstructions of m*edium spiny neurons* (MSN) in the *striatum* of aged Lrrk2-R1441C-KI (A) and Lrrk2-KD (B) mice. **C**,**D**) Quantification of selected morphological parameters. **E**,**F**) Sholl Analysis, depicting only slight tendencies towards an increase in branching and network complexity marked by subtle increasing numbers of higher order neurites in Lrrk2-KD animals (F). (Bar graphs represent the mean with standard error).
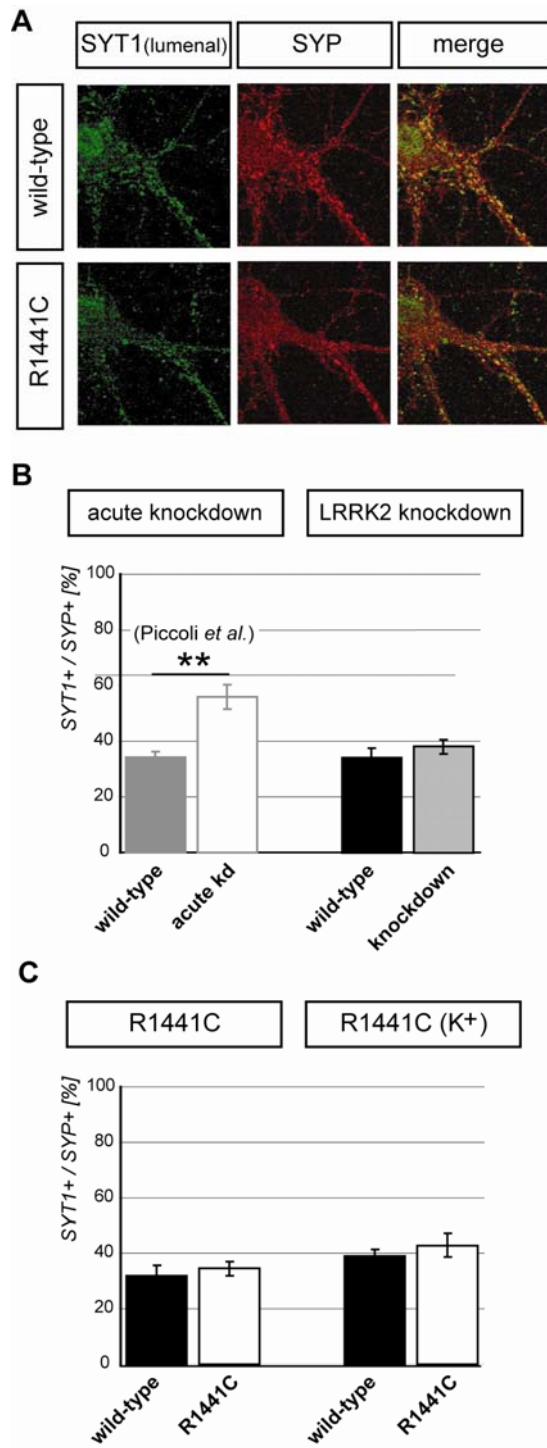
Figure 5: **Exo-/endocytosis assay demonstrate synaptic vesicle turnover alterations to be compensated in constitutive models. A**) Confocal picture of a hippocampal neuron stained for the luminal domain of *synaptotagmin 1* (Syt1),

representing the fraction of vesicles which underwent an endocytosis event during the time of the assay and *synaptophysin* (Syp), representing the total amount of synaptic vesicles in place. **B,C**) Quantification for hippocampal neurons prepared from Lrrk2-R1441C-KI mice under basal and potassium evoked conditions (K^+): Only the acute knockdown of Lrrk2 significantly increases the synaptic vesicle turnover (previously published data, (Piccoli et al., 2011)). Neither the constitutive loss of Lrrk2 protein in neurons prepared from the Lrrk2-KD line, nor the expression of mutated Lrrk2 on endogenous level (C) is sufficient t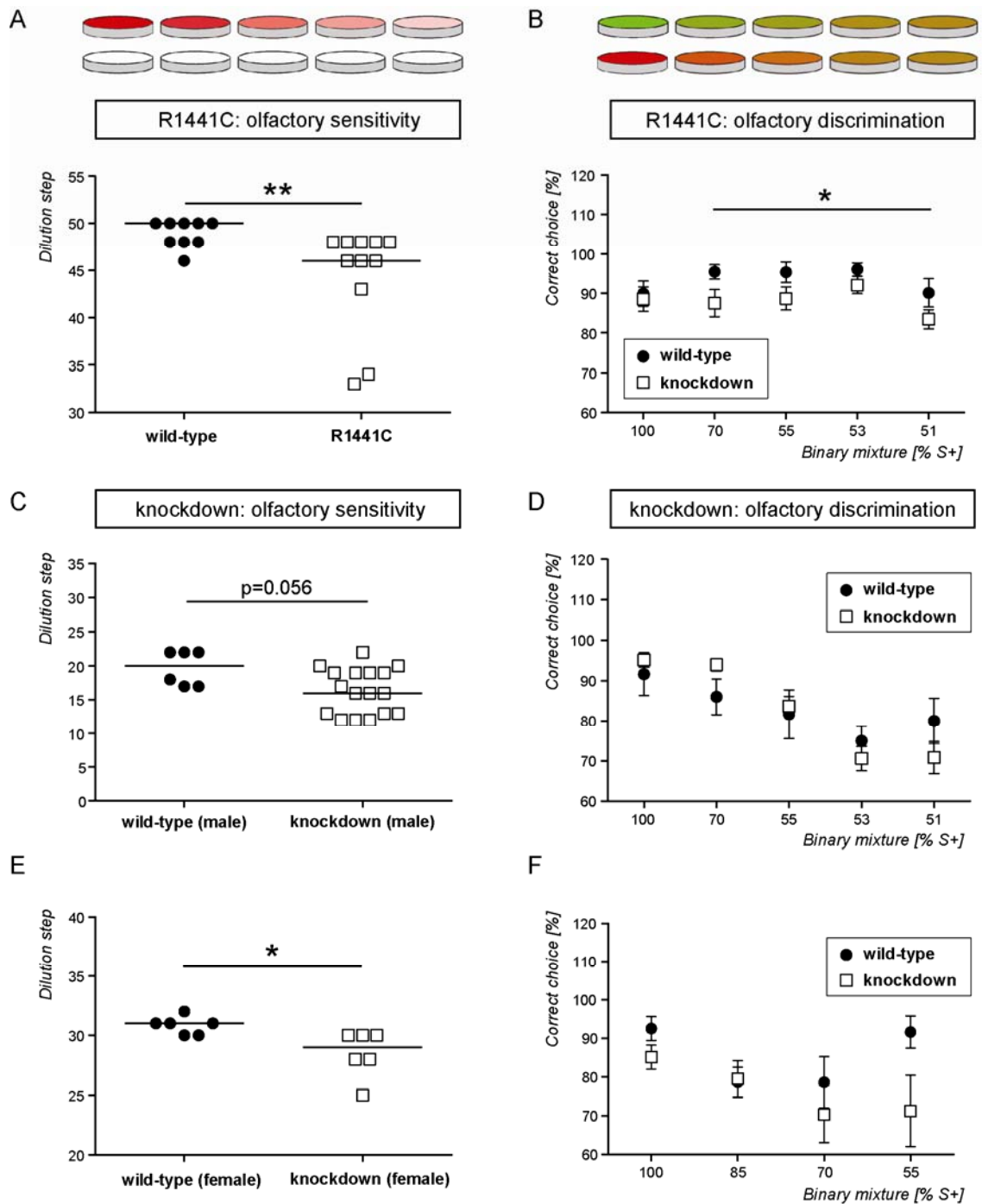o induce alterations in synaptic vesicle turnover (**$p<0.01$, bar graphs represent the Mean with Standard Error, $n>20$).

Figure 6: **Olfactory abilities are reduced in aged Lrrk2-R1441C-KI and Lrrk2-KD mice. A**) In the sensitivity assay, animals have to discriminate a conditioned odorant from the solvent. With increasing dilution, Lrrk2-R1441C-KI mice failed significantly more early, compared to their wildtype littermates. **B**) In the discrimination assay, animals are tested for their ability to discriminate binary mixtures of a conditioned

odor (red) and an unfamiliar odor (green). Lrrk2-R1441C-KI mice made less correct choices in different binary mixtures ($F_{(1,17)}$=5.685; P=0.029). **C**,**E**) In the sensitivity task, old male (C) Lrrk2-KDs show a trend towards reduced abilities. In the females (E) it is a significant difference (Females: t_{10}=2.7, P= 0.022; Males: U= 23.5; P=0.056). **D**,**F**) In the discrimination task, no differences between Lrrk2-KD groups were found. (Graphs represent the mean with standard error)
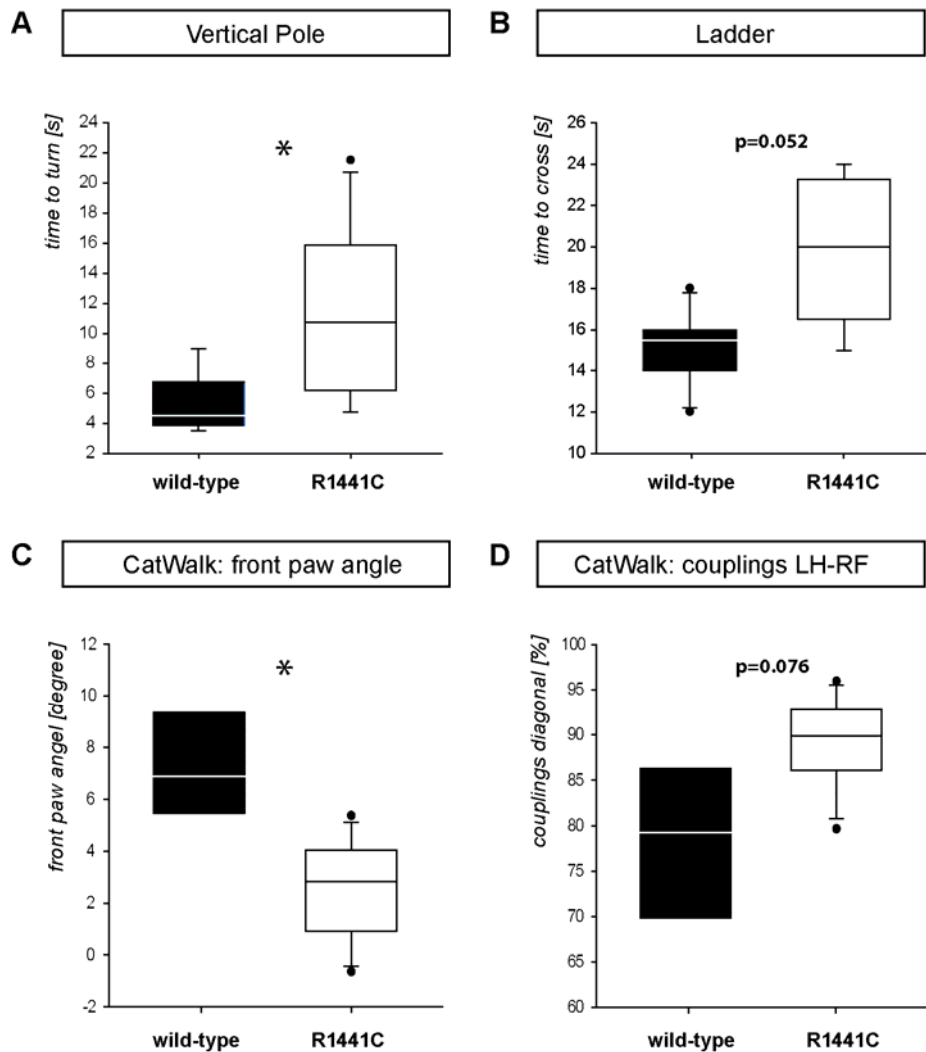
A Vertical Pole

B Ladder

C CatWalk: front paw angle

D CatWalk: couplings LH-RF

Figure 7: **Gait performance and motor abilities are diminished in Lrrk2-R1441C-KI animals.** Lrrk2-R1441C-KI mice took longer to turn on the Vertical Pole (A) and had an increased time to cross the Ladder (B). On the CatWalk® mutants showed alterations in front paw angle (C) and in diagonal couplings of the left hindpaw and the right frontpaw (D) (*p<0.05, Vertical Pole and Ladder test: 5 wild-type males: 5; mutant males 7; for the CatWalk® 4 wild-types and 8 mutants, box plots represent the 10th, 25th, 75th and 90th percentile with the median).
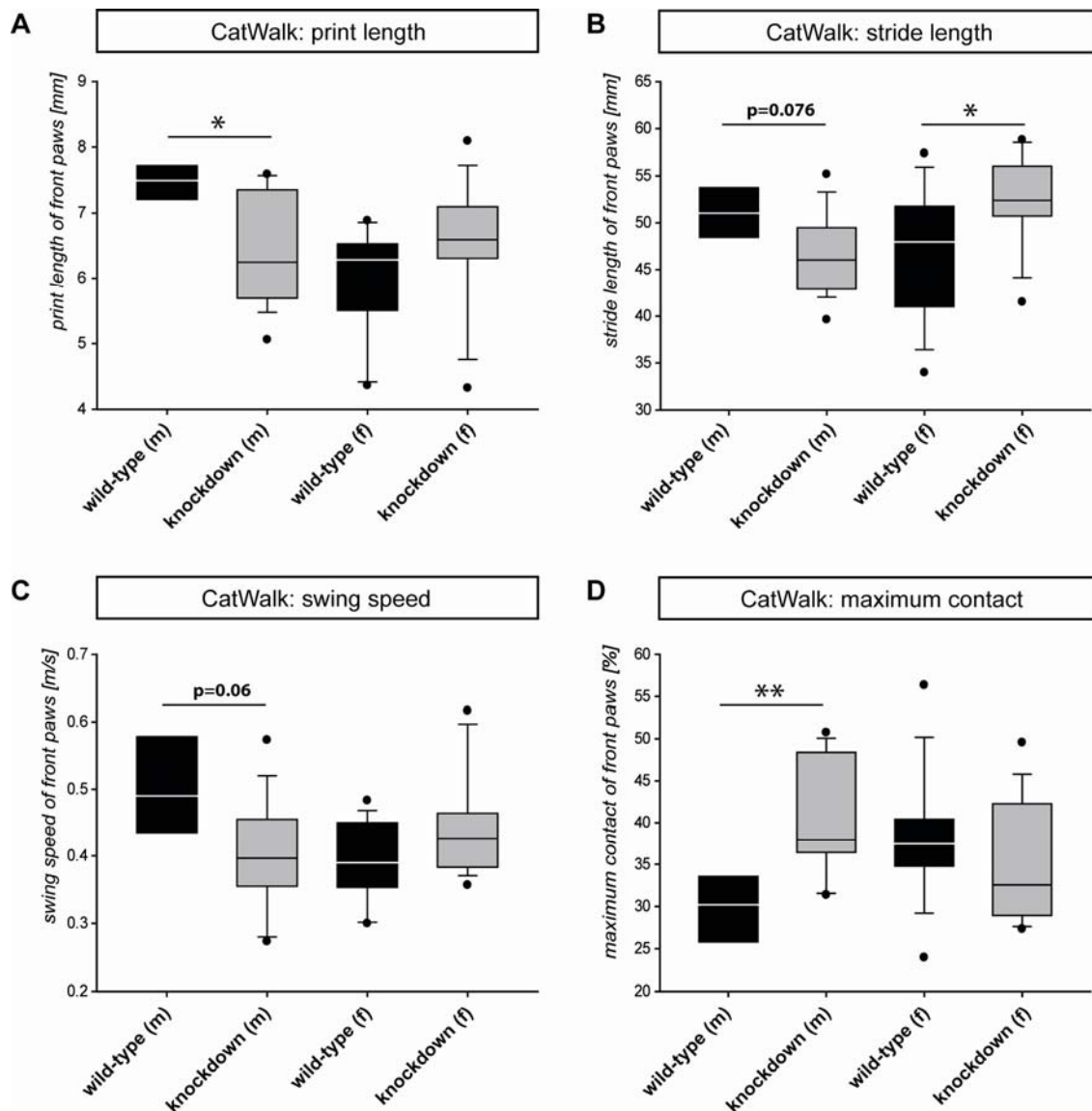
***Figure 8:*** **Gait impairments on the CatWalk in Lrrk2-KD.**

Lrrk2-KD animals show several alterations when analyzed in the CatWalk®. Significant sex- genotype interactions occur in the print length (A), stride length (B), swing speed (C) and maximum contact (D) of the front paws. Results from post hoc testing are depicted in the graphs (*p<0.05, **p<0.01, male wild-types: 4; male mutants: 15; female wild-type: 10; female mutants: 11; box plots represent the 10th, 25th, 75th and 90th percentile with the median).

Feature	Specification		R1441C	AGE	knockdown	AGE
Morphology	number of DA-neurons in SNpc		→	(5 and 28 month)	→	(28 month)
	innervation of the striatum		→	(5 and 28 month)	→	(28 month)
	Lewy body formation		→	(5 and 28 month)	→	(28 month)
	Tau-pathology		→	(5 and 28 month)	→	(28 month)
Dendritic morphology (MSNs)	neurite quantity		→	(12 month)	→	(12 month)
	overall neurite length		→	(12 month)	→	(12 month)
	neurite arborisation		→	(12 month)	→	(12 month)
Synaptic transmission	constitutive mutants		→	(14-21 DIV)	→	(14-21 DIV)
	acute knock-down		n.a.	(14-21 DIV)	↑*	(14-21 DIV)
Motor symptoms	Open field (motor aspects)		→	(10 weeks)	→	(14 weeks)
	Rotarod performance		→	(12 weeks)	→	(16 weeks)
	Grip strength		→	(>24 month)	→	(>24 month)
	Beam Walk (total slips)		↑*	(>24 month)	→	(>24 month)
	Ladder test (time to cross)		↑t	(>24 month)	→	(>24 month)
	Vertical Pole test (time to turn)		↑*	(26 month)	→	(25 month)
Non-motor symptoms	Olfactory function	sensitivity	↓*	(24-26 month)	↓*sex	(24 month)
		discrimination	↓*	(24-26 month)	→	(24 month)
	Gait	paw associated deficits	↑*	(26 month)	↑*sex	(24-27 month)
		leg coordination deficits	↑t	(26 month)	↑*sex	(24-27 month)
	Cognition	Object Recognition Test	→	(14 weeks)	→	(18 weeks)
	Anxiety	Open Field test	→	(10 weeks)	↓*	(14 weeks)
		Tail Suspension test	↓*	(31 weeks)	↓*	(49 weeks)
		Forced Swim test	↓*	(38 weeks)	→	(60 weeks)

Table 1: **Overview of PD associated symptoms in both Lrrk2 mouse lines.**

PD associated fine motor symptoms are exclusively visible in the Lrrk2-R1441C-KI line (indicated in orange). In addition, Lrrk2-R1441C-KI mice in comparison to the Lrrk2-KD animals show a higher degree of PD associated prodromal symptoms (indicated in green). Abbreviations: ↑,↓,→ up, down, not altered; *sex = only significant in one sex; n.d. = not determined; n.a. = not applicable; DIV = days *in vitro*.
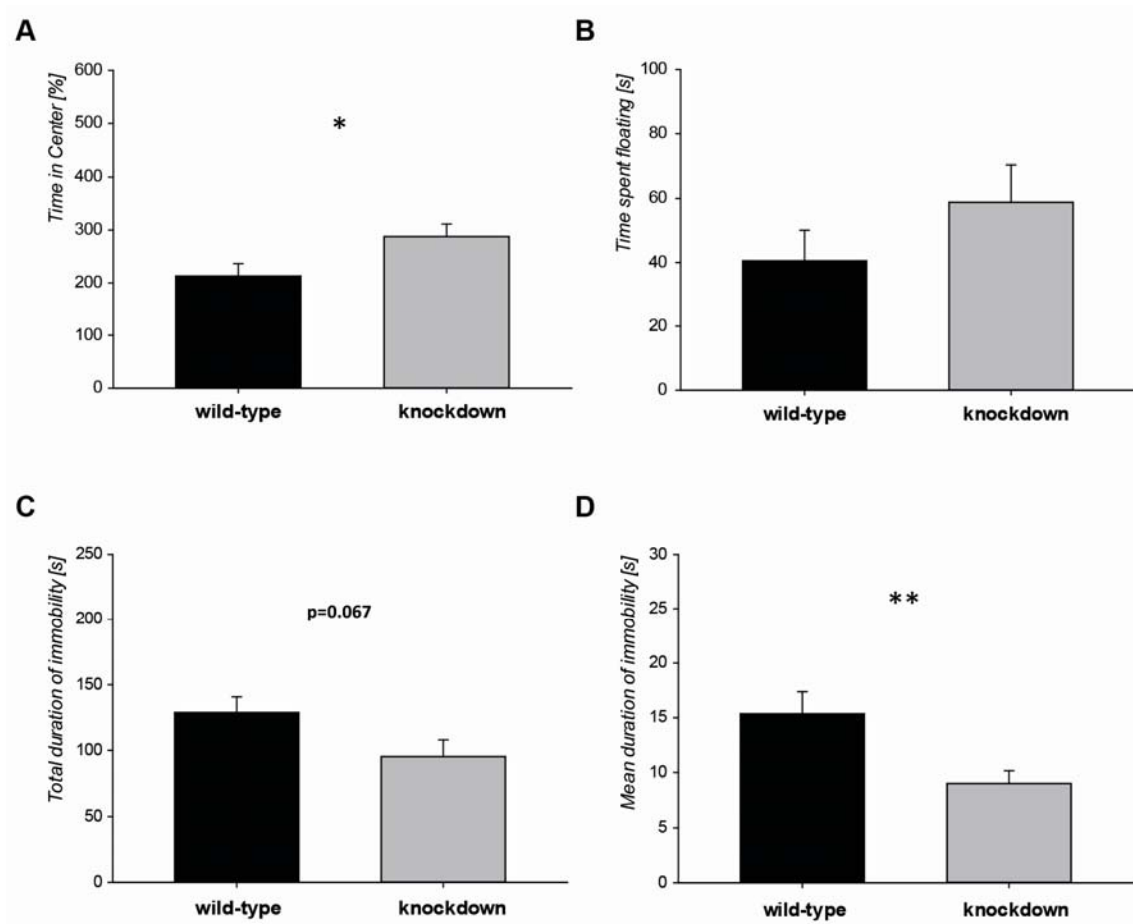
SUPPLEMENTS:
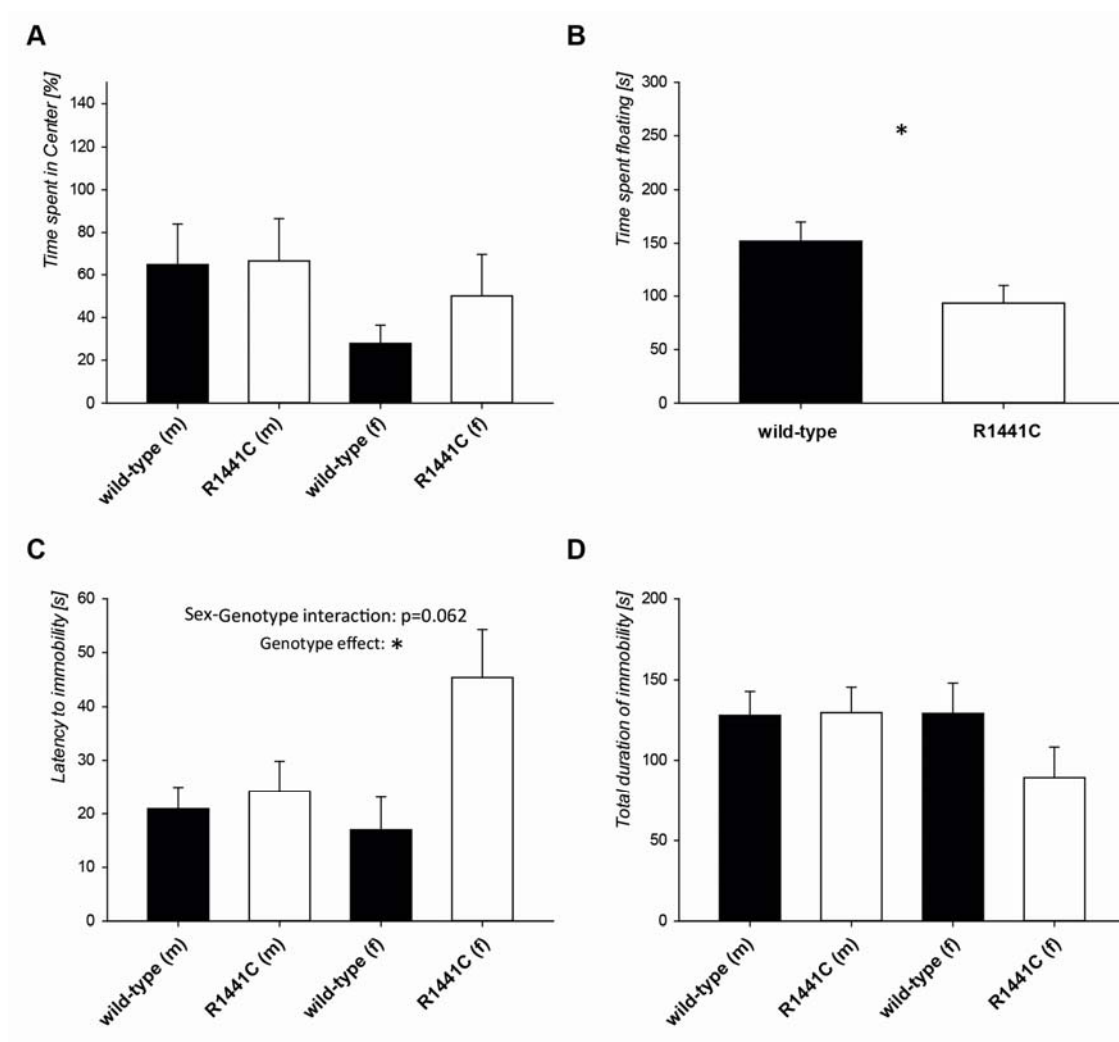
Supplement Figure S1: Lrrk2-R1441C-KI female mice show a reduced depression-related phenotype.

No significant effects in the Open Field test (A, n=8-15). Lrrk2-R1441C-KI animals spent less time floating in the Forced Swim test (B, n=8-12), indicating decreased depression-like behavior. This result is strengthened by the Tail Suspension test (n=9-13), where mutants demonstrated an increased latency to immobility compared to wild-type controls (C). No effects were seen in the total duration of immobility in

the Tail Suspension test (D) (*p<0.05, bar graphs represent the mean with standard

error).

Supplement Figure S2: Anxiety- and depression-related behavior is reduced in the Lrrk2-KD animals.

During the Open Field test (n=7-17), Lrrk2-KD mice spent significantly more time in the centre of the test arena (A) suggesting reduced anxiety. No genotype differences were revealed in the Forced Swim test (B; n=10-16). Results of the Tail Suspension test (n=10-18) demonstrated a reduction in the total (C) and mean (D) duration of immobility (*p<0.05, **p<0.01, bar graphs represent the mean with standard error).

References:

Alam, M., et al., 2011. The pedunculopontine nucleus area: critical evaluation of interspecies differences relevant for its use as a target for deep brain stimulation. Brain. 134, 11-23.

Andres-Mateos, E., et al., 2009. Unexpected lack of hypersensitivity in LRRK2 knock-out mice to MPTP (1-methyl-4-phenyl-1,2,3,6-tetrahydropyridine). J Neurosci. 29, 15846-50.

Bacci, A., et al., 2001. Chronic blockade of glutamate receptors enhances presynaptic release and downregulates the interaction between synaptophysin-synaptobrevin-vesicle-associated membrane protein 2. J Neurosci. 21, 6588-96.

Baltadjieva, R., et al., 2006. Marked alterations in the gait timing and rhythmicity of patients with de novo Parkinson's disease. Eur J Neurosci. 24, 1815-20.

Beccano-Kelly, D. A., et al., 2014a. Synaptic function is modulated by LRRK2 and glutamate release is increased in cortical neurons of G2019S LRRK2 knock-in mice. Front Cell Neurosci. 8, 301.

Beccano-Kelly, D. A., et al., 2014b. LRRK2 overexpression alters glutamatergic presynaptic plasticity, striatal dopamine tone, postsynaptic signal transduction, motor activity and memory. Hum Mol Genet. 24, 1336-49.

Begley, C. G., Ioannidis, J. P., 2015. Reproducibility in science: improving the standard for basic and preclinical research. Circ Res. 116, 116-26.

Berardelli, A., et al., 2001. Pathophysiology of bradykinesia in Parkinson's disease. Brain. 124, 2131-46.

Bergareche, A., et al., 2016. DAT imaging and clinical biomarkers in relatives at genetic risk for LRRK2 R1441G Parkinson's disease. Mov Disord. 31, 335-43.

Bichler, Z., et al., 2013. Non-motor and motor features in LRRK2 transgenic mice. PLoS One. 8, e70249.

Blanca Ramirez, M., et al., 2016. LRRK2 and Parkinson s disease: from lack of structure to gain of function. Curr Protein Pept Sci. epub ahead of print.

Bloem, B. R., et al., 2001. Postural instability and falls in Parkinson's disease. Adv Neurol. 87, 209-23.

Bosgraaf, L., Van Haastert, P. J., 2003. Roc, a Ras/GTPase domain in complex proteins. Biochim Biophys Acta. 1643, 5-10.

Braak, H., et al., 2003. Staging of brain pathology related to sporadic Parkinson's disease. Neurobiol Aging. 24, 197-211.

Braak, H., et al., 2004. Stages in the development of Parkinson's disease-related pathology. Cell Tissue Res. 318, 121-34.

Byler, S. L., et al., 2009. Systemic lipopolysaccharide plus MPTP as a model of dopamine loss and gait instability in C57Bl/6J mice. Behav Brain Res. 198, 434-9.

Chou, J. S., et al., 2014. (G2019S) LRRK2 causes early-phase dysfunction of SNpc dopaminergic neurons and impairment of corticostriatal long-term depression in the PD transgenic mouse. Neurobiol Dis. 68, 190-9.

Cryan, J. F., et al., 2005. Differential behavioral effects of the antidepressants reboxetine, fluoxetine, and moclobemide in a modified forced swim test following chronic treatment. Psychopharmacology (Berl). 182, 335-44.

Delic, S., et al., 2008. Genetic mouse models for behavioral analysis through transgenic RNAi technology. Genes Brain Behav. 7, 821-30.

Deng, X., et al., 2011. Characterization of a selective inhibitor of the Parkinson's disease kinase LRRK2. Nat Chem Biol. 7, 203-5.

Dickson, D. W., et al., 2009. Neuropathological assessment of Parkinson's disease: refining the diagnostic criteria. Lancet Neurol. 8, 1150-7.

Dranka, B. P., et al., 2013. Diapocynin prevents early Parkinson's disease symptoms in the leucine-rich repeat kinase 2 (LRRK2R(1)(4)(4)(1)G) transgenic mouse. Neurosci Lett. 549, 57-62.

Dranka, B. P., et al., 2014. A novel mitochondrially-targeted apocynin derivative prevents hyposmia and loss of motor function in the leucine-rich repeat kinase 2 (LRRK2(R1441G)) transgenic mouse model of Parkinson's disease. Neurosci Lett. 583, 159-64.

Dzamko, N., et al., 2010. Inhibition of LRRK2 kinase activity leads to dephosphorylation of Ser(910)/Ser(935), disruption of 14-3-3 binding and altered cytoplasmic localization. Biochem J. 430, 405-13.

Ebersbach, G., et al., 1999. Interference of rhythmic constraint on gait in healthy subjects and patients with early Parkinson's disease: evidence for impaired locomotor pattern generation in early Parkinson's disease. Mov Disord. 14, 619-25.

Farrer, M. J., 2006. Genetics of Parkinson disease: paradigm shifts and future prospects. Nat Rev Genet. 7, 306-18.

Forno, L. S., 1996. Neuropathology of Parkinson's disease. J Neuropathol Exp Neurol. 55, 259-72.

Frye, S. V., et al., 2015. Tackling reproducibility in academic preclinical drug discovery. Nat Rev Drug Discov. 14, 733-4.

Funayama, M., et al., 2002. A new locus for Parkinson's disease (PARK8) maps to chromosome 12p11.2-q13.1. Ann Neurol. 51, 296-301.

Gaenslen, A., et al., 2011. The patients' perception of prodromal symptoms before the initial diagnosis of Parkinson's disease. Mov Disord. 26, 653-8.

Gaig, C., et al., 2007. G2019S LRRK2 mutation causing Parkinson's disease without Lewy bodies. J Neurol Neurosurg Psychiatry. 78, 626-8.

Galter, D., et al., 2006. LRRK2 expression linked to dopamine-innervated areas. Ann Neurol. 59, 714-9.

Giasson, B. I., et al., 2006. Biochemical and pathological characterization of Lrrk2. Ann Neurol. 59, 315-22.

Giasson, B. I., Van Deerlin, V. M., 2008. Mutations in LRRK2 as a cause of Parkinson's disease. Neurosignals. 16, 99-105.

Giesert, F., et al., 2013. Expression analysis of Lrrk1, Lrrk2 and Lrrk2 splice variants in mice. PLoS One. 8, e63778.

Glasl, L., et al., 2012. Pink1-deficiency in mice impairs gait, olfaction and serotonergic innervation of the olfactory bulb. Exp Neurol. 235, 214-27.

Gloeckner, C. J., et al., 2010. Phosphopeptide analysis reveals two discrete clusters of phosphorylation in the N-terminus and the Roc domain of the Parkinson-disease associated protein kinase LRRK2. J Proteome Res. 9, 1738-45.

Haehner, A., et al., 2009. Olfactory dysfunction as a diagnostic marker for Parkinson's disease. Expert Rev Neurother. 9, 1773-9.

Haehner, A., et al., 2014. A clinical approach towards smell loss in Parkinson's disease. J Parkinsons Dis. 4, 189-95.

Healy, D. G., et al., 2008. Phenotype, genotype, and worldwide genetic penetrance of LRRK2-associated Parkinson's disease: a case-control study. Lancet Neurol. 7, 583-90.

Hinkle, K. M., et al., 2012. LRRK2 knockout mice have an intact dopaminergic system but display alterations in exploratory and motor co-ordination behaviors. Mol Neurodegener. May, 7-25.

Hughes, A. J., et al., 2001. Improved accuracy of clinical diagnosis of Lewy body Parkinson's disease. Neurology. 57, 1497-9.

Ito, G., et al., 2014. Lack of correlation between the kinase activity of LRRK2 harboring kinase-modifying mutations and its phosphorylation at Ser910, 935, and Ser955. PLoS One. 9, e97988.

Kordower, J. H., et al., 2013. Disease duration and the integrity of the nigrostriatal system in Parkinson's disease. Brain. 136, 2419-31.

Lavalley, N. J., et al., 2016. 14-3-3 Proteins regulate mutant LRRK2 kinase activity and neurite shortening. Hum Mol Genet. 25, 109-22.

Lesage, S., Brice, A., 2009. Parkinson's disease: from monogenic forms to genetic susceptibility factors. Hum Mol Genet. 18, R48-59.

Li, X., et al., 2010. Enhanced striatal dopamine transmission and motor performance with LRRK2 overexpression in mice is eliminated by familial Parkinson's disease mutation G2019S. J Neurosci. 30, 1788-97.

Li, X., et al., 2011. Phosphorylation-dependent 14-3-3 binding to LRRK2 is impaired by common mutations of familial Parkinson's disease. PLoS One. 6, e17153.

Li, Y., et al., 2009. Mutant LRRK2(R1441G) BAC transgenic mice recapitulate cardinal features of Parkinson's disease. Nat Neurosci. 12, 826-8.

Liu, H. F., et al., 2014. LRRK2 R1441G mice are more liable to dopamine depletion and locomotor inactivity. Ann Clin Transl Neurol. 1, 199-208.

Lobbestael, E., et al., 2013. Identification of protein phosphatase 1 as a regulator of the LRRK2 phosphorylation cycle. Biochem J. 456, 119-28.

MacLeod, D., et al., 2006. The familial Parkinsonism gene LRRK2 regulates neurite process morphology. Neuron. 52, 587-93.

Mamais, A., et al., 2014. Arsenite stress down-regulates phosphorylation and 14-3-3 binding of leucine-rich repeat kinase 2 (LRRK2), promoting self-association and cellular redistribution. J Biol Chem. 289, 21386-400.

Marsden, C. D., 1983. Neuromelanin and Parkinson's disease. J Neural Transm Suppl. 19, 121-41.

Matsuura, K., et al., 1997. Pole test is a useful method for evaluating the mouse movement disorder caused by striatal dopamine depletion. J Neurosci Methods. 73, 45-8.

Melrose, H., et al., 2006. Anatomical localization of leucine-rich repeat kinase 2 in mouse brain. Neuroscience. 139, 791-4.

Melrose, H. L., et al., 2010. Impaired dopaminergic neurotransmission and microtubule-associated protein tau alterations in human LRRK2 transgenic mice. Neurobiol Dis. 40, 503-17.

Mihalick, S. M., et al., 2000. An olfactory discrimination procedure for mice. J Exp Anal Behav. 73, 305-18.

Miller, J. D., et al., 2013. Human iPSC-based modeling of late-onset disease via progerin-induced aging. Cell Stem Cell. 13, 691-705.

Mirelman, A., et al., 2011. Gait alterations in healthy carriers of the LRRK2 G2019S mutation. Ann Neurol. 69, 193-7.

Muda, K., et al., 2014. Parkinson-related LRRK2 mutation R1441C/G/H impairs PKA phosphorylation of LRRK2 and disrupts its interaction with 14-3-3. Proc Natl Acad Sci U S A. 111, E34-43.

Nichols, R. J., et al., 2010. 14-3-3 binding to LRRK2 is disrupted by multiple Parkinson's disease-associated mutations and regulates cytoplasmic localization. Biochem J. 430, 393-404.

Nixon-Abell, J., et al., 2016. L'RRK de Triomphe: a solution for LRRK2 GTPase activity? Biochem Soc Trans. 44, 1625-1634.

Noyce, A. J., et al., 2016. The prediagnostic phase of Parkinson's disease. J Neurol Neurosurg Psychiatry. 87, 871-8.

Ogawa, N., et al., 1985. A simple quantitative bradykinesia test in MPTP-treated mice. Res Commun Chem Pathol Pharmacol. 50, 435-41.

Paisan-Ruiz, C., et al., 2004. Cloning of the gene containing mutations that cause PARK8-linked Parkinson's disease. Neuron. 44, 595-600.

Paisan-Ruiz, C., et al., 2013. LRRK2: cause, risk, and mechanism. J Parkinsons Dis. 3, 85-103.

Parisiadou, L., et al., 2014. LRRK2 regulates synaptogenesis and dopamine receptor activation through modulation of PKA activity. Nat Neurosci. 17, 367-76.

Pham, T. T., et al., 2010. DJ-1-deficient mice show less TH-positive neurons in the ventral tegmental area and exhibit non-motoric behavioural impairments. Genes Brain Behav. 9, 305-17.

Piccoli, G., et al., 2011. LRRK2 controls synaptic vesicle storage and mobilization within the recycling pool. J Neurosci. 31, 2225-37.

Pont-Sunyer, C., et al., 2015. Sleep Disorders in Parkinsonian and Nonparkinsonian LRRK2 Mutation Carriers. PLoS One. 10, e0132368.

Postuma, R. B., et al., 2012. How does parkinsonism start? Prodromal parkinsonism motor changes in idiopathic REM sleep behaviour disorder. Brain. 135, 1860-1870.

Prut, L., Belzung, C., 2003. The open field as a paradigm to measure the effects of drugs on anxiety-like behaviors: a review. Eur J Pharmacol. 463, 3-33.

Rajput, A., et al., 2006. Parkinsonism, Lrrk2 G2019S, and tau neuropathology. Neurology. 67, 1506-8.

Reynolds, A., et al., 2014. LRRK2 kinase activity and biology are not uniformly predicted by its autophosphorylation and cellular phosphorylation site status. Front Mol Neurosci. 7, 54.

Ruiz-Martinez, J., et al., 2011. Olfactory deficits and cardiac 123I-MIBG in Parkinson's disease related to the LRRK2 R1441G and G2019S mutations. Mov Disord. 26, 2026-31.

Saunders-Pullman, R., et al., 2014. Olfactory identification in LRRK2 G2019S mutation carriers: a relevant marker? Ann Clin Transl Neurol. 1, 670-8.

Shulman, L. M., et al., 1996. Internal tremor in patients with Parkinson's disease. Mov Disord. 11, 3-7.

Siderowf, A., Lang, A. E., 2012. Premotor Parkinson's disease: concepts and definitions. Mov Disord. 27, 608-16.

Simon-Sanchez, J., et al., 2006. LRRK2 is expressed in areas affected by Parkinson's disease in the adult mouse brain. Eur J Neurosci. 23, 659-66.

Spillantini, M. G., et al., 1997. Alpha-synuclein in Lewy bodies. Nature. 388, 839-40.

Steckler, T., 2015. Preclinical data reproducibility for R&D--the challenge for neuroscience. Psychopharmacology (Berl). 232, 317-20.

Steru, L., et al., 1987. The automated Tail Suspension Test: a computerized device which differentiates psychotropic drugs. Prog Neuropsychopharmacol Biol Psychiatry. 11, 659-71.

Tagliaferro, P., et al., 2015. An early axonopathy in a hLRRK2(R1441G) transgenic model of Parkinson disease. Neurobiol Dis. 82, 359-71.

Tepper, J. M., Bolam, J. P., 2004. Functional diversity and specificity of neostriatal interneurons. Curr Opin Neurobiol. 14, 685-92.

Tong, Y., et al., 2009. R1441C mutation in LRRK2 impairs dopaminergic neurotransmission in mice. Proc Natl Acad Sci U S A. 106, 14622-7.

Tong, Y., et al., 2010. Loss of leucine-rich repeat kinase 2 causes impairment of protein degradation pathways, accumulation of alpha-synuclein, and apoptotic cell death in aged mice. Proc Natl Acad Sci U S A. 107, 9879-84.

Trullas, R., et al., 1989. Genetic differences in a tail suspension test for evaluating antidepressant activity. Psychopharmacology (Berl). 99, 287-8.

Tsika, E., et al., 2015. Adenoviral-mediated expression of G2019S LRRK2 induces striatal pathology in a kinase-dependent manner in a rat model of Parkinson's disease. Neurobiol Dis. 77, 49-61.

Ujiie, S., et al., 2012. LRRK2 I2020T mutation is associated with tau pathology. Parkinsonism Relat Disord. 18**,** 819-23.

Volta, M., et al., 2015. Chronic and acute LRRK2 silencing has no long-term behavioral effects, whereas wild-type and mutant LRRK2 overexpression induce motor and cognitive deficits and altered regulation of dopamine release. Parkinsonism Relat Disord. 21**,** 1156-63.

Wefers, B., et al., 2012. MAPK signaling determines anxiety in the juvenile mouse brain but depression-like behavior in adults. PLoS One. 7**,** e35035.

Weng, Y. H., et al., 2016. (R1441C) LRRK2 induces the degeneration of SN dopaminergic neurons and alters the expression of genes regulating neuronal survival in a transgenic mouse model. Exp Neurol. 275 Pt 1**,** 104-15.

Wurst, W., 2016. Animal Models Are Valid to Uncover Disease Mechanisms. PLoS Genet. 12**,** e1006013.

Yuan, R., et al., 2009. Aging in inbred strains of mice: study design and interim report on median lifespans and circulating IGF1 levels. Aging Cell. 8**,** 277-87.

Zimprich, A., et al., 2004. Mutations in LRRK2 cause autosomal-dominant parkinsonism with pleomorphic pathology. Neuron. 44**,** 601-7.